Highlights

Regionally-synchronous climate change during the LG-IT in SW Asia

Clear vegetation response to shifts in climate, but with some time lags

^{14}C-date probability distributions show different demographic trends between regions

Demographic and environmental continuity through the Younger Dryas in the Levant

This was not the case in upland Anatolia, which experienced a later Neolithic onset

Human responses and non-responses to climatic variations during the Last Glacial-Interglacial transition in the eastern Mediterranean

Paper for QSR MEDINES Special Issue

Neil Roberts[1], Jessie Woodbridge[1], Andrew Bevan[2], Alessio Palmisano[2], Stephen Shennan[2] and Eleni Asouti[3]

1. *School of Geography, Earth and Environmental Sciences, Plymouth University, PL4 8AA, UK*
2. *Institute of Archaeology, University College London*
3. *Department of Archaeology, Classics and Egyptology, University of Liverpool*

Email: cnroberts@plymouth.ac.uk

Abstract

We review and evaluate human adaptations during the last glacial-interglacial climatic transition in southwest Asia. Stable isotope data imply that climatic change was synchronous across the region within the limits of dating uncertainty. Changes in vegetation, as indicated from pollen and charcoal, mirror step-wise shifts between cold-dry and warm-wet climatic conditions, but with lag effects for woody vegetation in some upland and interior areas. Palaeoenvironmental data can be set against regional archaeological evidence for human occupancy and economy from the later Epipalaeolithic to the aceramic Neolithic. Demographic change is evaluated from summed radiocarbon date probability distributions, which indicating contrasting – and in some cases opposite - population trajectories in different regions. Abrupt warming transitions at ~14.5 and 11.7 ka BP may have acted as pacemakers for rapid cultural change in some areas, notably at the start of the Natufian and Pre-Pottery Neolithic cultures. However temporal synchroneity does not mean that climatic changes had the same environmental or societal consequences in different regions. During cold-dry time intervals, regions such as the Levant acted as refugia for plant and animal resources and human population. In areas where socio-ecological continuity was maintained through periods of adverse climate (e.g. Younger Dryas) human communities were able to respond rapidly to subsequent climatic improvement. By contrast, in areas where there was a break in settlement at these times (e.g. central Anatolia), populations were slower to react to the new opportunities provided by the interglacial world.

Keywords: Southwest Asia, Neolithic revolution, agricultural origins, palaeo-demography, charcoal, pollen

1. Introduction

Southwest Asia is one of the earliest and most important global centres of plant and animal domestication. From the Neolithic farmers of this region we have inherited cereal crops (wheat, barley, rye), pulses (pea, lentil), and domestic animals (sheep, goat, pig, cattle) (Zohary and Hopf, 2001; Colledge et al., 2004; Conolly et al., 2011). The increased economic productivity and new social organization associated with this 'Neolithic revolution' during the early Holocene were associated with population growth, increased sedentism and the beginnings of village life (Barker, 2006). It has long been hypothesised that the beginnings of Neolithic agriculture in southwest Asia were in some way connected to the major shift in global climate at the end of the last Ice Age (Bar-Yosef, 2017). In this paper we firstly review the historical development of ideas about human adaptations in the eastern Mediterranean during the last glacial-interglacial transition from ~16,000 to ~9000 Cal. yr BP. We then evaluate the current evidence for climatic and ecological change from both off-site and on-site contexts in the eastern Mediterranean region, including stable isotope geochemistry, fossil pollen and charcoals. These are compared against regional archaeological evidence for human occupancy and population change from the late Epi-Palaeolithic to the end of the aceramic Neolithic. Demographic evidence for cultural continuity or discontinuity is evaluated from summed radiocarbon date probability distributions. Finally, we critically compare the archaeological and palaeoenvironmental data sets in order to assess human responses and non-responses to changes in the natural environment.

Archaeological sites in the eastern Mediterranean region older than c. 12 ka BP (12,000 Cal. yr BP) belong to Epipalaeolithic cultures, such as the Natufian of the southern Levant. Sites were relatively small and most were only occupied seasonally. Many site economies included harvesting of wild cereal stands, while others involved exploitation of wild herds of sheep, goat and gazelle. In both cases these formed part of broadly based economies utilizing a wide range of resources (Hillman, 1996; Harris, 1998; Rosen and Rivera-Collazo, 2012). During the earliest aceramic Neolithic (Pre-Pottery Neolithic A or PPNA, ~11.7-10.5 ka BP) there are clear indications of cultivation of morphologically wild cereals, for example at the site of Jerf el Ahmar in the Euphrates valley (Willcox and Stordeur 2012). By the later pre-pottery Neolithic (=PPNB, ~10.5-9.0 ka BP) fully-fledged farming villages had appeared widely throughout the so-called Fertile Crescent, and indeed beyond it into central Turkey. Sites were much larger, reflecting communities whose populations were numbered in hundreds or even thousands, and whose mode of production was rapidly becoming based on agriculture (Goring-Morris and Belfer-Cohen 2008).

Sites of domestication for founder crops appear to have been restricted to the Fertile Crescent (Nesbitt, 2002). There is good bio-molecular and archaeobotanical evidence that single-grained einkorn wheat was domesticated in the Karaca Dağ volcanic uplands of southeast Turkey during the first 1,500 years of the Holocene (Heun et al., 1997; Willcox, et al. 2009). However, bio-archaeological evidence indicates that the crop domestication process was not

restricted to this core area (Fuller et al., 2012). For instance, morphologically-domestic emmer wheat appears early in the Damascus basin to the south and also further north near the middle reaches of the river Tigris at Çayönü, and the same is true for barley (Colledge et al., 2004). This suggests the possibility of multiple independent domestication events for cereal grasses. The first domestic sheep and goat appear at about the same time as these large-grained cereal crops (Conolly et al., 2011), with the earliest dated bio-archaeological evidence coming from the Zagros mountains of western Iran and northeastern Iraq (Zeder and Hesse, 2000; Riehl et al., 2013).

This evidence shows that the change from a mobile, hunter-gatherer economy to sedentary agriculture in southwest Asia was not instantaneous, but involved a long transitional period that created new selection pressures on the crops concerned, leading to increased frequencies of domestication traits, and with considerable variation in individual site economies (Zeder, 2011). It may have been the greater commitment to farming indicated by the emergence of large nucleated communities in the later PPNB that led to the crop packages that are familiar to us, and which became linked to developing practices of animal husbandry (Asouti and Fuller, 2012). The package of livestock and grain crops was subsequently 'exported' from Southwest Asia into adjacent areas, especially north-westwards to form the basis of traditional European subsistence farming.

2. The role of climate change in the transition to agriculture in the Eastern Mediterranean region: a brief historiography

The broad chronological coincidence between plant and animal domestication and the shift in global climate at the end of the last ice age has long offered a tempting explanatory framework for the emergence of agriculture. One of the first and best known theories relating climatic change to domestication for the eastern Mediterranean region was proposed by V.G. Childe in his book *The Most Ancient East* (1928). At that time it was believed that high latitude glacial periods were accompanied by lower latitude pluvials or wet phases (e.g. Brooks 1926; see also Butzer, 1958; Horowitz, 1979). The Late Pleistocene Lisan Formation in the Dead Sea basin provided field evidence of former high lake levels that was used to support this glacial-pluvial correlation. Raphael Pumpelly had previously inferred that Old World landscapes had witnessed a progressive drying out, or desiccation, with water resources increasingly concentrated in locally favoured habitats in river valleys and around lakes (Goudie 1973). In these few 'oases' Pumpelly (1908, pp.65-66) postulated that plants, animals and humans were forced to reside in close proximity on a reduced resource base, conditions that led to new relationships in the form of domestication. Pumpelly's oasis hypothesis was related to his archaeological and geological discoveries in central Asia rather than southwest Asia, and he offered no proper timescale for when cereal domestication might have begun. His ideas were clearly framed within an "environmental determinist" paradigm that was prevalent in Geography and other disciplines at the start of the twentieth century. Childe (1928), following Peake and Fleure (1927), transferred Pumpelly's oasis - or propinquity - hypothesis to the Near East, and added a clear archaeological chronology, in what he termed the 'Neolithic agricultural revolution'. On the

other hand, Childe did not view the emergence of Neolithic farming in Southwest Asia and/or Egypt during the early post-glacial period as climatically pre-determined. Rather he argued that it was one among several strategies adopted in the face of environmental change, in line with possibilist approaches to nature-culture relations that prevailed at that time.

Systematic archaeological field research into the origins of agriculture in southwest Asia only began in the late 1940s and 1950s with the work of R. Braidwood, K. Kenyon and others. Excavations of "tell" sites such as Jarmo and Jericho revealed Neolithic villages that were dated by the new radiocarbon method back to the very start of the Holocene. These excavations showed that whereas Childe had been correct in dating his Neolithic Revolution to near the beginning of the Holocene, he had been wrong to place it in Mesopotamia or the Lower Nile. Most early Neolithic sites such as Jarmo lie away from major alluvial river valleys, often in the hilly flanks of the Fertile Crescent (a term first proposed by J.H. Breasted in his book of the same name (1916)). Excavated mudbrick dwellings contained charred seeds, whose subsequent analysis, notably by archaeobotanist H. Helbaek, showed many of them to be early domestic cereals significantly different from naturally occurring wild varieties.

Braidwood was anxious to investigate the climatic background to the emergence of Neolithic farming, and as part of his field research in Iraqi Kurdistan invited American geologist H.E. Wright to accompany him in the field. Wright's fieldwork focussed initially on evidence for past glaciation in the Zagros mountains (Wright, 1962). At first Braidwood and his associates came to the conclusion that there had been no significant climatic changes in Southwest Asia during the last ~15 millennia that could explain the emergence of agriculture (Reed and Braidwood 1960). However, as Wright (1980, p.145) later admitted, these initial conclusions were largely based on lack of hard evidence for the Late Glacial-early Holocene period, and that evidence was not long in coming. In 1960, Wright crossed from Iraqi to Iranian Kurdistan in order to core Zeribar, a small lake close to the frontier (Fig. 1). According to ^{14}C dating these sediment cores represented a continuous record of environmental change over more than 18 ka (i.e. since before the Last Glacial Maximum). Wright collaborated with Dutch palynologist/archaeobotanist W. van Zeist at Groningen, and also with limnologist G.E. Hutchinson at Yale for geochemical analyses. The results (van Zeist and Wright, 1963; Hutchinson and Cowgill, 1963; Wright 1968) represented the first serious test of the hypothesized climatic explanation for Childe's 'Neolithic Revolution'. Pollen analysis showed that instead of the present-day oak parkland, the Zeribar region was a treeless chenopod-*Artemisia* steppe during the late Pleistocene, a flora typical of cold dry climatic conditions, not one with a "pluvial" climate. Further pollen studies in Southwest Asia have confirmed the Zeribar sequence (van Zeist and Bottema, 1991) and they indicate a sequence of climatic and vegetation changes that was the reverse of that predicted by the oasis hypothesis. The early Holocene witnessed a gradual re-establishment of woodland vegetation, indicating higher precipitation, not climatic desiccation. The geochemical data from Zeribar were in broad agreement with the pollen evidence in indicating lower lake levels and a drier climate in the earlier part of the record. They also represented a pioneering

example of the multi-proxy approach that is now widely adopted in studies of past environmental change (Lotter 2003) and they encouraged Hutchinson and Cowgill to carry out subsequent coring work and multi-proxy sediment analyses at Lake Hula in Israel (Cowgill, 1969).

Thus, rather than contracting, the availability of environmental resources increased in most areas of the eastern Mediterranean during the Glacial-Interglacial transition. And rather than early Holocene oases, it would have been in glacial-age refugia where plants, animals and humans would have been squeezed together. Wild cereals, for example, were common only in a few areas of the Mediterranean during glacial times, and Wright (1976) suggested that parts of North Africa, such as Morocco, might have been significant wild cereal refugia during the late Pleistocene. Although subsequent research has shown this not to be true for the Maghreb, glacial-age environmental conditions were relatively favourable in some areas of North Africa, such as Cyrenaica (Prendergast et al., 2016). Overall evidence indicates that the most important glacial refuge area for wild cereals was in the southern Levant, an area that was less adversely affected by Late Pleistocene cold and aridity. Increases in temperature and rainfall during the Late Glacial and early Holocene then allowed wild cereal grasses to expand from here to occupy their present-day distribution over the Fertile Crescent (Wright, 1993).

Although the abandonment of a simple glacial-pluvial correlation has meant that the oasis theory as originally formulated is no longer tenable, it has re-emerged in a much reduced and modified version. This is because expansion of the plant and animal resources required for domestication was halted, or even reversed, just prior to the "Neolithic Revolution", by the climatic deterioration of the Younger Dryas stadial (~13.0 – 11.7 ka BP). Working at the Epi-Palaeolithic/ Neolithic site of Tell Abu Hureyra on the middle Euphrates, A. Moore and G. Hillman (1992) found evidence for declining availability of wild cereals and pulses at the time of the Younger Dryas. They were replaced at this time by other wild plant resources such as chenopods. Moore and Hillman proposed that reduced availability of wild cereals and other plant foods at this time might have acted as the stimulus for new forms of human resource use, with climatic deterioration acting as a trigger for subsequent crop domestication (but see Colledge and Conolly, 2010).

What is clear from the above review is that major climatic and environmental changes occurred during the last Glacial-Interglacial transition, even if the Pumpelly-Childe "oasis" hypothesis is no longer tenable. It is therefore not possible to exclude climatic changes from any comprehensive model purporting to explain the emergence of agriculture in the eastern Mediterranean region.

3. A reconstruction of climate and vegetation during the last glacial – interglacial transition

In this section we review and analyse data sets for climatically-induced environmental change between the Last Glacial Maximum (LGM) and ~9 ka BP in the eastern Mediterranean region. Initially we focus on stable isotope records

from cave carbonates (speleothems), and from lake and deep marine sediments, supplemented by other evidence, such as lake-level and mountain glacier fluctuations. We then go on to synthesise and evaluate changes in vegetation and land cover, primarily from pollen analysis along with plant macrofossil data, particularly charcoals.

3.1. Stable isotope records of hydro-climate

Stable isotope data have responded rapidly and sensitively to changes in climate and water balance, and they represent a valuable "common currency" for climatic reconstruction. Although their precise significance varies between different natural archives and – in some cases – between sites (cf. Roberts et al 2008), stable isotopes offer one of the best ways to provide a synthetic overview of shifts in climatic conditions in the region during the last glacial – interglacial transition. Data come principally from stable isotope analysis of oxygen ($\delta^{18}O$) and carbon ($\delta^{13}C$) on endogenic or biogenic carbonates from caves, lakes and the sea. Cave speleothems now provide some of the best isotopic records from southwest Asia, many of which come from the Levant (e.g. Bar-Matthews et al., 1997; Frumkin et al., 1999; Verheyden et al., 2008), thus overlapping geographically with a key area of archaeological importance. Speleothem growth itself implies hydrological activity and hence periods when effective water was available (Vaks et al., 2006). Lake isotopic records are widely distributed across the eastern Mediterranean although causal controls vary between sites, depending mainly on the degree of hydrological lake closure. Mediterranean lake isotope data were synthesised by Roberts et al (2008), to which can be added records from Yammouneh in Lebanon (Develle et al., 2010) and Nar lake in central Anatolia (Dean et al., 2015). Stable isotope analysis of foraminiferal tests from East Mediterranean deep sea cores (e.g. Emeis et al., 2000) provide a means of linking terrestrial records to the global marine isotope stratigraphy and to North Atlantic palaeoceanography, although they generally offer a lower stratigraphic resolution than caves and some lakes.

Some of the key isotopic records are shown in figure 2 and listed in table S1, with site locations in figure 1. During the last glacial – interglacial transition all these records show a shift from more positive to more negative isotopic values. For $\delta^{18}O$, this shift is partly due to deglacial changes in the isotopic composition of source waters in the oceans (Kolodny et al., 2005), a shift that was amplified in the eastern Mediterranean Sea by meltwater discharge from the Eurasian ice sheet via the Black Sea. Correcting by 1-2 per mille for lower Sea Surface Temperatures (Almogi-Labin et al., 2009) surface waters in the eastern Mediterranean Sea were isotopically heavier than at present by around 2-3 per mille, that is, more than the 1-2 per mille ice volume effect found in the world oceans. However, changes in $\delta^{18}O$ in lake and cave records cannot be explained by source area composition effects alone (Almogi-Labin et al., 2009). A significant part was also caused by changes in regional hydro-climate, as reflected in the positive co-variance between $\delta^{18}O$ and $\delta^{13}C$ in records from many lakes (Roberts et al., 2008) and caves (Bar-Matthews et al., 1997; Cheng et al., 2015). Thus the overall regional hydro-climatic trend between the LGM and the early Holocene was one of increasing moisture availability, in line with the

climatic conditions inferred from the pollen record at Zeribar. This long-term isotopic trend was, however, interrupted by a Late Glacial climatic reversal that separated two periods of rapid climate warming/wetting. The eastern Mediterranean isotope curves closely resemble the climate-stratigraphic sequence from the north Atlantic region, summarised by the Greenland ice core record (Fig. 2). On the other hand, the apparent timing of isotopically-inferred climatic changes varies between individual eastern Mediterranean sequences. The apparent lack of synchrony between climate phases even led S. Bottema (1995) to question whether southwest Asia experienced a phase equivalent to the Younger Dryas stadial at all.

The weight of evidence now strongly suggests that apparent differences in the timing of climate change between different sites, both for stable isotopes and for pollen (discussed below), are primarily due to a lack of dating precision and accuracy. Firstly, sequence chronologies are based on a range of different dating methods, including ^{14}C, U-Th and varve counts, and these may not be directly commensurable. Many of the older studies have relatively few dates, often with conventional ^{14}C rather than AMS dates (e.g. Zeribar), and sometimes with large statistical uncertainties (e.g. Eski Acıgöl). At some sites (e.g. Hula; Meadows 2005) there were substantial old carbon distortions of apparent ^{14}C ages, while changes in the Mediterranean marine ^{14}C reservoir correction are imperfectly known. Secondly, those sites with the most detailed and internally consistent chronologies show a much smaller range of age variations and a better match to the Greenland ice core ages. This applies especially to cave records such as Sofular and Jeita that are dated by U-series using mass spectrometry (Göktürk et al., 2011, Cheng et al., 2015). Thirdly, it is possible to identify some proxy-climate indicators that must have changed synchronously across the region, and thus provide time-marker horizons. M. Rossignol-Strick (1995) adopted this approach using key pollen taxa in marine and terrestrial records – such as chenopod pollen - to show that the apparent age of the Younger Dryas (=G-S1) stage was in error at sites such as Hula. In similar vein, shifts in the portion of the $\delta^{18}O$ signal caused by changes in source water composition must be the same age across the region, and can thus be used to correlate between records. (This does not apply to the Black Sea, however, whose oxygen isotope stratigraphy is different from that of the Mediterranean Sea; this in turn influenced sites such as Sofular cave, whose $\delta^{18}O_r$ came mainly from this northern source (Bahr et al., 2006; Göktürk et al., 2011)). Overall, we can infer that within the "normal" limits of dating precision (i.e. ± 200-500 years), climatic changes appear to have been synchronous across the eastern Mediterranean between ~16 and ~9 ka BP and in tune with those in the wider Mediterranean and the North Atlantic, a conclusion in line with that of Robinson et al. (2006). On the other hand, these climatic shifts would not have had the same impact across the eastern Mediterranean region.

In order to explore further climate trends during the last Glacial-Interglacial transition, multiple isotope records listed in table S1 have been statistically normalised to create z-scores (following Roberts et al. 2011), and time-averaged for each of the major climate phases, which are assumed to have been synchronous across the region. These allow an assessment of how much of the

glacial-to-interglacial change in climate was accomplished during the initial warming/wetting step equivalent to the Bölling/Alleröd (GI-1) interstadial, and how far the subsequent Younger Dryas (GS-1) put this climatic amelioration into reverse. As shown in figure 3, some of the coldest and/or driest climatic conditions were coincident with the North Atlantic Heinrich 1 event (~16-17 ka BP), in line with other Heinrich events that correspond to phases of cold and aridity in the eastern Mediterranean (Bartov et al., 2003). The only exception to this is Lake Van, whose glacial-age $\delta^{18}O$ record fails to register the positive isotopic values found at other sites at that time, possibly because of isotopically-light meltwater from surrounding mountain glaciers (Kwiecien et al., 2014).

During the first period of climatic amelioration (=Bölling/Alleröd interstadial, ~13-15 ka BP), normalised $\delta^{18}O$ values show a rather large range of variation between records (Fig. 3). At some sites (e.g. Eski Acıgöl, Soreq, Sofular) isotopic values at this time were close to or even above those during the early Holocene, implying analogous climatic conditions. However, in other records the normalised isotopic change is only around 40-50% of that achieved by the early Holocene. In some cases (e.g. marine cores) this may be linked to "smoothing" of the trend due to bioturbation or mixed isotope sources. Normalised $\delta^{18}O$ values are more tightly clustered during the subsequent climatic reversal (=Younger Dryas stadial, 11.7-13 ka BP), with values between a quarter and a half of the full glacial-interglacial climatic range, except at Lake Van and at Dim Cave. In other words, inferred climatic conditions at this time appear to have been less severely cold and dry than at the time of the H1 event, in line with similar findings elsewhere in the world (Meltzer and Bar-Yosef, 2012). During the second phase of climatic amelioration at the start of the Holocene (~11.7 ka BP), conditions improved rapidly to within 20% of those in full early Holocene times (~10-8.5 ka BP) which coincided with the formation of eastern Mediterranean Sapropel 1. The data in figure 3 show no clear spatial patterns, although there is a suggestion that the Younger Dryas climate reversal led a larger drop in temperatures and moisture availability in upland interior areas (e.g. Lake Van). The overall mean isotopic values indicate that around two-thirds of the glacial-interglacial shift in climate was accomplished during the initial step (H1 to B/A), with a subsequent return to values about one-third of the full shift during the Younger Dryas climate reversal. The second warming/wetting step at the start of the Holocene was similar in amplitude to the first, but probably with higher absolute values of temperature and precipitation. Significantly, as in the Greenland ice record (Grootes and Stuiver 1997), both of the major warming steps (~14.5 and 11.7 ka BP) appear to have been extremely rapid in Southwest Asia. At Van, Eski Acıgöl and at Nar, whose lake sediment records are laminated, most of the isotopic shift at the start of the Holocene took place in less than a century according to laminae counts (Wick et al., 2003; Roberts et al., 2001; Dean et al., 2015). At Eski Acıgöl, this is also true for the isotope shift marking the onset of the "Bölling/Alleröd" interstadial. These abrupt and sustained shifts in climate, with mean temperatures rising by up to 1°C per decade, had dramatic consequences for environmental resource availability and would have been felt directly within an individual human lifetime.

While there is now broad agreement about the timing and phasing of climatic change during the last Glacial-Interglacial transition in Southwest Asia, some other research issues of palaeoclimatic reconstruction remain less clearly resolved. One issue (discussed in section 3.1, below) relates to the explanation for pollen evidence of a slow re-advance of trees across interior areas of Anatolia and western Iran during the early Holocene. Another issue concerns the hydro-climatic interpretation of Late Pleistocene high lake levels, notably in the Dead Sea basin. As previously noted, the deep-water lake Lisan that occupied the lowest part of the Jordan rift in glacial times was a key line of evidence in the glacial-pluvial correlation that is now discredited for Southwest Asia as a whole. There remain contrasting views about whether glacial-age high lake levels in Southwest Asia were the result of a cold-dry or a cool-moist climate (e.g. Enzel et al., 2008; Gasse et al., 2014; Stockhecke et al., 2016), as both scenarios could have caused lake water levels to rise. It is unlikely that some areas of Southwest Asia received an increase in precipitation while other areas nearby experienced an absolute precipitation fall, in a kind of localised climatic see-saw. Glacial-age high lake levels occurred across the region, for example in central Anatolia (Roberts et al., 1999), not just in the Dead Sea basin. None the less, it is clear that precipitation gradients between coastal and interior areas of Southwest Asia were more marked at the LGM than they have been during the Holocene. This is evident in glacier palaeo-equilibrium lines reconstructed from cosmogenically-dated moraines. They show, for example, that Sandıras Dağ near the coast of southwest Turkey was glaciated to elevations around 1000 m lower than Mount Erciyes in interior Anatolia (Sarıkaya et al., 2008, 2009). This can only have been due to much higher precipitation on coastal mountains than inland, a conclusion supported by evidence for important glacial-age forest refugia in the coastal uplands, compared to herb-steppe on the Anatolian plateau (see below). Overall, coastal and more southerly areas of the eastern Mediterranean were less severely affected by the cold-dry climate at, and immediately after, the LGM, than were upland, interior regions. Areas such as the southern Levant therefore maintained relatively favourable conditions for lake water balance, for plant growth and for human occupation even at times of adverse climate, such as during the H1 event.

3.2 Changes in vegetation and land cover

3.2.1 Pollen records

Pollen analysis represents the most comprehensive way to reconstruct changes in regional vegetation. However, it should be borne in mind that pollen percentage data do not take account of differential production, dispersal and preservation between individual taxa. Indeed some plant taxa, such as *Amygdalus* (almond) are not represented at all in the pollen record. Partly because of this, as well as assessing regional changes in pollen assemblages we also compare them against woody plant taxa recorded in charcoals from archaeological sites spanning the Late Glacial – early Holocene transition. Most pollen sites in southwest Asia come from lakes or wetlands located in climatically wetter areas, often in uplands, while drier/lowland areas are not so well represented, although these were often important archaeologically. The

problems of dating precision and accuracy (discussed above) also apply to pollen records; in fact, some of the lake isotope and pollen data derive from the same sites and/or cores.

We focus here on pollen sequences that span most or all of the time period between 16 and 9 ka BP from those parts of Southwest Asia where crop and animal domestication took place (Fig. 1). Ten of the main pollen records have been put on a common calendrical timescale in order to facilitate comparison between them. Five of these sites derive from Anatolia and Northwest Iran, while another five sites come from the Levant (see Table S2 for details). Figure 4 summarises changes at each site in three major plant groups; 1) steppic herbs (*Artemisia*+chenopodiaceae), 2) grasses (including cereal-type) and 3) broad-leaf trees, of which oak (*Quercus*) is most important. As figure 4a shows, there was an overall decrease in herb steppe vegetation across the region during the glacial-interglacial climatic transition. At several sites (e.g. Akgöl (Konya), Urmia and al-Jourd), there was an initial decline in *Artemisia*, chenopods or both, followed by a secondary increase, and then by a more permanent decline at the start of the Holocene, typically between 12 and 11 ka BP. Chenopodiaceae remained significant at some sites during the early Holocene, although this group of taxa also includes pollen from local halophytic plants that commonly grow around salt lakes such as Urmia. At many sites, the grass pollen curve (Fig. 4b) shows a reverse trend to that of steppic herbs, with an overall increase over time, although often fluctuating. There was a significant phase of grass-steppe dominance during the opening millennia of the Holocene, especially across the upland regions of central-east Anatolia and northwest Iran. This is commonly associated with micro-charcoal influx peaks, implying that wildfires helped to maintain an open grassland landscape at this time (Turner et al., 2008). The proportion of pollen of broad-leaf trees, especially deciduous oak, also increased during the glacial-interglacial transition, primarily during the early Holocene rather than late Pleistocene (Fig. 4c). Whereas this expansion occurred quite fast in most lowland pollen records from the Levant (e.g. Ghab, Huleh), the increase in oak pollen was rather slow in upland interior areas, and at some sites (e.g. Zeribar) maximum *Quercus* values were only achieved as late as 6 ka BP. There has been extensive discussion in the literature about whether the delayed re-advance of woodland was caused by climatic controls (e.g. Stevens et al., 2001; Djamali et al., 2012), by ecological dynamics slowing the spread of trees (e.g. van Zeist and Bottema, 1991), by human factors such as burning and grazing (e.g. Roberts, 2002), or some combination of these different agencies (Roberts et al., 2011). What is clear is that by the 10th millennium BP, bio-archaeological evidence for aceramic Neolithic resource use implies that oak parklands were being actively managed and altered (Asouti and Kabukcu, 2014). There was not only a contrast in the timing of woodland expansion between coastal and interior regions of Southwest Asia, but also in overall woodland cover, which was denser in wetter, coastal areas than it was in drier interior plateaux, such as around Lake Urmia and on the Konya plain of south central Anatolia.

In addition to these major ecosystems, some other areas of Southwest Asia were characterised by an expansion in needle-leaf forests of pine, cedar and fir, for example around Lake Beyşehir in southwest Anatolia (Bottema and Woldring

1984). Another vegetation type that became significant during the early Holocene was *Pistacia* (terebinth) parkland. This small tree is a low pollen producer and so is under-represented in pollen diagrams (Fig. 4d), but it is clear that *Pistacia* was a significant component of many of Southwest Asia's semi-arid landscapes during the early Holocene (see further discussion below).

This pattern of vegetation change is consistent with the sequence of Late-Glacial climatic changes described in section 3.1 above, although there is some variation in the timing of changes from site to site. For example, the early Holocene decline in *Artemisia* and chenopods has a calculated age as early as 12.2 ka BP at some sites (e.g. Eski Acıgöl) but as late as 10.5 ka BP at others (e.g. Urmia). However the mean age for this vegetation change across all sites corresponds quite closely to the established date for the Younger Dryas-Holocene climatic transition at 11.7 ka BP.

3.2.2 Charcoal data

Macro-charcoals from archaeological deposits provide a valuable complement to pollen records in terms of regional vegetation history, as well as for understanding past human use of woody plant resources (Asouti and Austin, 2005). Unlike micro-charcoals, they are identifiable to genus, and they can also be dated directly by radiocarbon. On the other hand, the wood was collected and selected deliberately by people, and this is likely to have introduced some cultural taphonomic bias into the eventual charcoal assemblage that was preserved. For example, at Epi-Palaeolithic Wadi Faynan site 16 in southern Jordan, a dominance of *Juniperus* rather than *Pistacia* wood (whose nutshell was ubiquitous in the archaeobotanical samples) may reflect a site-specific cultural preference for the use of locally available juniper old wood as timber and fuel (Mithen et al., 2007).

For this paper we have drawn on published syntheses for the southern Levant (Asouti et al., 2015) and south central Turkey (Asouti and Kabukcu, 2014). Along with these we have put together quantitative charcoal count data for a number of archaeological sites in the northern Fertile Crescent, to which can be added non-quantified data for a number of other sites, such as Körtik Tepe and Abu Hureyra. Details of the charcoal data can be found in table S3 and summary charts in figure 5. For these charts, count data were grouped into five time phases and regional averages calculated (see table S4 for details).

For the southern Levant, the regional anthracological record suggests that vegetation and climate were substantially different from the present-day during the Late Glacial and early Holocene. In the only pre-Natufian site for which data are available (Nahal Neqarot), charcoals were dominated by *Juniperus*, a taxon that is absent today from the Negev Highlands (Baruch and Goring-Morris, 1997). Juniper remained a significant component of the southernmost Levantine vegetation until post-Neolithic times, and by the Late Natufian (≅Younger Dryas) it was joined by *Pistacia* and in the early Holocene by *Amygdalus/Prunus.* Deciduous oak only became a significant component of the wood charcoal assemblages in the mid-late PPNB, i.e. after ~10 ka BP, and evergreen oak was

only ever a minor component. Early Holocene (Neolithic) charcoal assemblages are notably more species-diverse than those of the late Pleistocene, including riparian taxa (e.g. Salicaceae, *Tamarix, Fraxinus*). The Late Glacial vegetation of the southern Levant would thus have been dominated by *Pistacia* savanna and *Juniperus–Pistacia* steppe woodlands to the east and south of the Jordan valley; this graded into *Pistacia–Amygdalus–Rhamnus–Prunus*–Maloideae moist woodland steppe and deciduous *Quercus* woodland that grew in moister localities, especially to the north and west of the Jordan valley, during the opening millennia of post-glacial times.

Further north, charcoal data for sites in the Irano-Anatolian foothills and mid-elevation slopes are absent until PPNA times. From the start of the Holocene, a broad diversity of woody taxa is represented, especially riparian trees/shrubs and *Pistacia*, along with deciduous oak and *Amygdalus/Prunus*, but not *Juniperus*. Rosaceae-dominated grasslands would have prevailed at the onset of the Holocene, including a small but distinct component of deciduous *Quercus* (Asouti and Kabukcu, 2014). In south central Anatolia, late-glacial Epi-Palaeolithic charcoal assemblages from Pınarbaşı in the Konya basin were dominated by *Amygdalus/Prunus* and *Juniperus*, with oak charcoals notably absent. By the time of the early Holocene human occupation of the Pınarbaşı rockshelter, juniper had been replaced by *Pistacia.* In contrast, around broadly the same time at Boncuklu in the middle of the Konya plain wetland, charcoals were dominated by riparian taxa (notably Salicaceae). Riparian trees were also important in the initial occupation levels at Çatalhöyük (early ceramic Neolithic in date), but these were quickly replaced by deciduous oak and – in the later levels – by juniper.

The charcoal assemblages summarised in figure 5 therefore reflect spatial variations at both local and regional scales, as well as long-term temporal trends, and they include a number taxa that are rare or absent in pollen records, such as *Amygdalus/Prunus* and *Celtis*. Juniper tolerates cold winter temperatures, and because of this it is relatively abundant in some charcoal assemblages of Late Glacial age and/or in upland contexts (e.g. Konya basin). However, juniper was also a significant element of wood charcoals at some sites of early Holocene age, possibly as an early-colonising tree. Southwest Asian juniper species are shade-intolerant and able to tolerate low-nutrient soils. A complex spatio-temporal pattern is also true of juniper in pollen records. *Juniperus* is significant in Late Glacial pollen assemblages from Lake Beyşehir (Bottema and Woldring, 1984), but is uncommon in sites from elsewhere in southwest and central Anatolia from this time period. At Van, a high elevation lake in eastern Anatolia, juniper was rare in Late Glacial and early Holocene times, and became a significant component of the regional vegetation only in the last five millennia as the climate became drier and soils more degraded (Wick et al., 2003).

In contrast to juniper, some other tree taxa display more coherent behaviour across southwest Asia since the LGM, at least partly because of climatic constraints. Deciduous oak, for example, is rare in both pollen and charcoal records of Late Glacial age, and both types of archive show that it increased in abundance during the early Holocene – albeit rather gradually - linked to

climatic amelioration, ecological dynamics (including wildfire and grazing), and human management for fuel, fodder and timber. *Pistacia* is another tree/shrub that expanded its range substantially in southwest Asia during the last glacial-interglacial climatic transition. Charcoal evidence shows that in the Negev this expansion began during the Late Glacial period (Fig. 5, tables S3 and S4). An expansion of *Pistacia* during the Late-Glacial interstadial is also recorded in some pollen records from the Levant (e.g. Al-Jourd; Cheddadi and Khater, 2016) and eastern Anatolia (e.g. Van; Wick et al., 2003), although this trend was reversed during the subsequent Younger Dryas stadial (Fig. 4d). eThe main phase of regional *Pistacia* dominance, however, occurred during the early Holocene, as first recognised by Rossignol-Strick (1995). *Pistacia* is a low pollen producer, so percentage values need to multiplied by ~10 for comparison with other tree taxa, such as oak; if this is done, there is then a good overall match between the pollen and charcoal *Pistacia* data (2-5% vs 20-50%). In marine pollen records, the *Pistacia* phase coincides with the S1 sapropel layer, which Rossignol-Strick (1995, 1999) suggested was indicative of warmer winter temperatures than in recent times. This phase is also found in many terrestrial pollen records, for example, in eastern Anatolia/northwest Iran (e.g. Van, Zeribar) and south central Anatolia (e.g. Eski Acıgöl and Nar; see Roberts et al., 2016, figure 8), where it is dated between ~11 and ~7 ka BP. This time period therefore witnessed a dramatic expansion of *Pistacia* parkland with grass understory, an ecosystem that dominated the vegetation of southwest Asia's semi-arid zone throughout the Neolithic.

4. Demographic changes in southwest Asia

There have been previous attempts to infer human population trends in Southwest Asia for the period of the late Pleistocene and early Holocene. Guerrero et al. (2008, fig. 2) used Bocquet-Appel's (2002) method of evaluating the juvenility index from age distributions of skeletons as a proxy for population growth. They found evidence of population growth in the earlier Natufian and population stabilization in the late Natufian, with a high rate of growth returning in the Pre-Pottery Neolithic (PPN). However, the chronological resolution of the data was low and the method provides information on growth rates, rather than relative population levels. The latter was attempted by Goring-Morris and Belfer-Cohen (2010, fig 4.2), who provided estimates of site densities per thousand years covering the period from the Upper Palaeolithic to the beginning of the Pottery Neolithic for five different regions of mainland southwest Asia. Both the Mediterranean southern Levant and the Tigris-Euphrates area show fairly constant rates of increase over the period, from very low initial levels, resulting in site densities of c.90 and 60 sites/thousand years respectively by the end of the period. The arid southern Levant and the Transjordanian desert show fluctuating patterns, the former with its highest peak, c.90 sites/thousand years, in the Middle Epipalaeolithic and the latter, c.65 sites/thousand years, in the late PPNB. For the northern Levant the pattern was rather flat, but with a trebling of the density from Late to Final PPNB, reaching a peak of c.35 sites/thousand years. Overall, there is some suggestion of a higher rate of increase with the arrival of farming but it is not marked. However, these patterns too are very low

in resolution and certainly provide no basis for investigating whether there is any connection with climate change.

To address this situation we have created a new population proxy for the period using summed calibrated radiocarbon probabilities. For this purpose, we have collected 1,917 ^{14}C dates from several major existing date collations (Böhner and Schyle 2002-2006; Maher et al., 2011; Borrell et al., 2015; Flohr et al., 2016) and a wide range of other published sources, over a slightly broader time range of 17 to 7.5 ka uncal in order to avoid edge effects. Using the resulting date list we have carried out both an overall analysis of all the relevant dates from Southwest Asia and an analysis on three regional subsets, 1) southern and central Levant, 2) northern Levant and Upper Mesopotamia, and 3) South-central Anatolia, to see if there are regional differences in population patterns (see fig. 6)[1].

Although reservations have often been expressed about the validity of summed radiocarbon probabilities as a population proxy, they have been consistently shown to correlate with other lines of evidence where these are available (e.g. Woodbridge et al., 2014; Lechterbeck et al., 2014; Crema et al., 2016). Our method largely follows the one laid out by Shennan et al. (2013) and Timpson et al. (2014) and provides means of taking into account the effect of the calibration curve and variation in the sample size on the resulting patterns. We reduce the bias that is potentially introduced by the over-sampling of certain site sequences by clustering uncalibrated dates from the same site that are within 50 years of each other and rescaling the overall weight of these neighbours' probability distributions, before summing probability distributions across different sites. This admittedly does not take into account site size and, insofar as there is considerable evidence for an increase in average site size over time (e.g. Kuijt 2000, Borrell et al., 2015), at least until the end of PPNB, the results are likely to underestimate the population trend for the later parts of the period.

A decision has to be made about the calibration method used, and in particular about whether dates are normalized prior to summation. For the dataset as a whole Fig 7a shows the summed distribution with each date normalized prior to summation (the method used by OxCal and others), showing an exacerbation of calibration curve artefacts in the form of spiked probability densities corresponding to the steepest portions of the calibration curve. Fig 7b shows the unnormalised results for the same dataset (the method used by CalPal). Following the discussion in Weninger et al. (2015), we have opted to use the unnormalised results in what follows as likely to give a better picture of the summed calibrated distribution. Figures 7a-b also show the impact of adjusting the IntCal13 curve according to improved tree-ring calibration for this period provided by Hogg et al (2016): in this case, there is little evidence for a major difference and so we have continued using IntCal13 for what follows.

In order to indicate where certain portions of the time series depart from baseline expectations, we fit an exponential model to the observed SPD (fig 7b)

[1] the full analysis and radiocarbon dataset are available at UCL Discovery repository at: http://dx.doi.org/10.14324/000.ds.1570274

and use it to simulate conditional-random SPDs, and calculate where the observed time series departs significantly from this model (as implemented by Crema et al., 2016). A different choice of fitted time range (e.g. 16-0 ka cal BP) will lead to different model residuals and observed deviation, but the overall trend within the chosen time range (16-9 ka cal BP) is well-summarised via an exponential curve. Substantively, this is also the pattern we would expect for long-term population increase over the period if it simply continued trends already established in the Epipalaeolithic. Departures from the trend potentially inform us about deviations from the long-term growth pattern but need to be distinguished from calibration curve effects that can also cause such deviations. This is made possible by simulating the exponential model a large number of times together with the calibration curve effects for the period concerned while also taking into account the sample size of available dates, to produce a 95% critical envelope for the model. Residuals falling outside that envelope can be considered extreme, and therefore potentially indicate departures from the exponential pattern, implying periods of population growth higher than the long-term trend, or of population decline. However, we cannot be sure of this because 5% of the time the exponential model will itself generate values outside the envelope, so we also calculate a global significance value by comparing the overall distribution of the data residuals to the results generated by the model.

Fig 7c shows the SPDs for the data and the 95% envelope for the exponential model for the time range 16-9 ka cal BP. The observed time series shows some significant overall departures from the envelope for the exponential model (global p-value=0.004). This is primarily a result of two periods where the population proxy for Southwest Asia as a whole lies outside the modelled range. The first of these occurs at 13.6-12.7 ka cal BP, corresponding to the temperature decline in the latter part of the Bølling-Allerød interstadial and the beginning of the Younger-Dryas, when inferred population levels fall below the envelope of "expected" values. The ^{14}C time series then rises rapidly to lie within the exponential trend interval by ~12.5 ka, well before the end of the Younger Dryas. From the end of the Younger Dryas at 11.7 ka until 11.1 ka BP, corresponding to the beginning of the Holocene and the early PPNA, inferred population is higher than predicted by the exponential model. In other words, the demographic trend from 12.7 ka to 11.6 ka suggests a continuous period of population growth through the Younger Dryas and into the Holocene, resulting in a 5-fold population increase over 1,100 years. This is in keeping with Flannery's (1969) long-standing suggestion that increased dependence on sustainable plant resources leads to people having more children (cf. Bocquet-Appel, 2002; Winterhalder and Goland, 1993). In fact, that increase levels off rapidly after the beginning of the Holocene c. 11.6 ka and continues flat until c.10.7 ka.

Figure 8 shows the regionally subdivided results, again unnormalised, for which the sample sizes are obviously greatly reduced, especially for south central Anatolia. The extent to which each sub-region departs from the pan-regional trend is tested via permutation of the regional labels (following the method outlined in Crema et al., 2016). All regions show significant departures (p-value ≤ 0.005) from the pan-regional pattern despite the reduced sample sizes. For the southern Levant (Fig. 8a) the main departure is in the period c.14.5-13.5 ka,

roughly corresponding to the onset of the Bølling-Allerød interstadial and the Early Natufian when population is significantly higher than the overall pattern (Maher et al., 2011, 14-15). In this region there appears to be a brief period of population growth in the middle of the Younger Dryas (—12.6 ka BP), but this then levelled off up to —12.0 ka when there was renewed increase until 11.3 ka, at which point a limit seems to have been reached. In total, this last increase represents "only" a doubling of population, assuming that site sizes remained constant.

In contrast, the population proxy for the Northern Levant/Upper Mesopotamia region (Fig. 8b) is significantly below the pan-regional pattern throughout the period 16.0-13.4 ka BP, at which point it starts a consistent upward trend that continues throughout the Younger Dryas to reach values that significantly exceed the global pattern from 11.7 until ~10.5 ka BP, after which it declines. In fact, between 13.4 and 11.5 ka BP population in the northern Levant grows roughly 20-fold. This region represents the main driver of the whole Southwest Asian pattern described above, with nearly 2000 years of major population growth before a peak is reached not long after the start of the Holocene. Perhaps significantly (see below), all of the sites in this region ^{14}C-dated to the time of the Younger Dryas lie at intermediate elevations, between 300 and 850 masl, that include the northern hilly flanks of the Fertile Crescent. The population peak at the end of the growth phase corresponds to the PPNA (Borrell et al. 2015, table 1) and coincides with the first clear archaeo-botanical evidence of cereal cultivation. It is obviously not coincidental that this is also the context for the appearance of the remarkable monuments at such sites as Göbekli Tepe, which can plausibly be viewed a response to the new and rapidly transformed high-density social-environmental world. From c. 10.3 ka, it appears that a short period of rapid decline led to a period of flat population lasting until 9.5 ka when growth returned. Although this falls within the pan-regional confidence interval of a slowly increasing trend during this period, it is in keeping with Borrell et al.'s (2015) claims for a settlement hiatus in the region 10.2 - 9.8 ka BP and contrasts with the suggestion of rapid growth in the southern Levant at this time (see also Kuijt 2008, 292-296).

Despite the much smaller number of ^{14}C dates and sites, and the resulting wider 95% confidence interval for the pan-regional pattern (Fig. 8c), south-central Anatolia still shows a globally significant difference from the long-term exponential trend (p=0.001). There is a period of c. 500 years from c. 15.2 ka when the overall population pattern is significantly exceeded but more noteworthy is the period from c. 12.7 to 11.2 ka BP, most of the Younger Dryas and the first 500 years of the Holocene, when population is flat and lies below the pan-regional confidence interval, a pattern that recurs briefly from c. 10.6 to 10.3 ka. By contrast, from 10.3 to 10.1 ka BP very rapid increase to a higher population level appears to occur in south-central Anatolia, contrasting with the apparent demographic decline already noted in the Northern Levant during the same period and possibly suggesting out-migration from one region to the other. Given that most of this variation falls within the confidence interval for the combined regions, these suggestions should be treated with caution, but it is important to note that the significant population peak in the south central

Anatolian region corresponds to the earliest occurrence of Neolithic "packages" such as sedentism, housing and proto-domestication of animals and plants at sites such as Boncuklu (Baird et al., 2012) and Aşıklı Höyük (Stiner et al., 2014; Berger et al. 2016). Conversely, the long period of low and flat population over the period 12.7-10.3 ka in south-central Anatolia provides little evidence that it formed part of the core area where cultivation first began. It is also noteworthy that except for two Epi-Palaeolithic cave sequences near to the coast, all the ^{14}C-dated archaeological sites in south central Anatolia lie at relatively high elevations, above ~1000 masl.

5. Analysis and Discussion

A number of previous studies have examined the relationship between climatic and archaeological changes during the Last Glacial-Interglacial transition in Southwest Asia (e.g. Robinson et al., 2006; Makarewicz, 2012, Meltzer and Bar-Yosef, 2012), but without clear agreement. For example, Blockley and Pinhasi (2011) concluded that the onset of some the principal archaeological phases (Natufian, PPNA) coincided with, and therefore could be seen as a response to, the key Northern Hemisphere warming events (start of the Bølling-Allerød interstadial and Younger Dryas-Holocene transition, respectively). By contrast, using a very similar radiocarbon data set from archaeological sites, Maher et al. (2011) came to a different conclusion that no clear correlation could be demonstrated between climatic and cultural changes. Henry (2013) also concluded that the start of the Late Natufian probably preceded the onset of the Younger Dryas by around 500 years, and therefore cannot be seen as a direct response to climatic deterioration.

In fact, it is difficult to resolve the issue of temporal synchronism with statistical rigour, because of uncertainties in the precision and accuracy of the relevant age data sets. The start of the Holocene is dated by layer counting of the Greenland ice cores as 11,703 calendar years before AD 2000, with a 99 year uncertainty at >95% probability (Walker et al., 2009). The statistical error on multiple archaeological ^{14}C dates is time-variable (as discussed in section 4), partly because the ^{14}C calibration curve is non-linear, but is not better than ±200 yr at 2 SDs for this region and time period. The statistical uncertainty on the dating of most proxy climate records from southwest Asia is even larger, partly because a wide range of dating methods have been used and also because shifts in climate proxies are not normally dated directly; instead their ages have to be interpolated between dated layers. For the majority of palaeoclimatic and pollen records discussed in sections 3.1 and 3.2, chronological precision for the start of the Holocene can be estimated as no better than ±500 yr at 2 SDs. It is consequently not possible to demonstrate that the temperature rise at the start of the Holocene in Greenland (±100 yr) and in the eastern Mediterranean (≥±500 yr) were synchronous with a high degree of statistical probability. However, similarity in the shape of proxy data curves and our understanding of Northern Hemisphere climate dynamics would give strong support to such a correlation. In the same way, linking the proxy-climate records from either Greenland or the eastern Mediterranean to ^{14}C date series for archaeological cultural phases is only possible with an uncertainty of several centuries. None the less, it would be

surprising if the largest and fastest changes in temperature and precipitation to have occurred during the last 20 ka had not prompted some new human lifeways in southwest Asia. The global climate shifts at ~14.5 and 11.7 ka BP were significantly larger in amplitude than that 8.2 ka BP, for example, and also lasted much longer (>1 ka cf. <200 yr), with societal impacts that would have hard to avoid. The dating evidence is therefore consistent with the hypothesis that these two periods of rapid climate change and new material cultures occurred at the same time, even if this cannot be proved statistically.

Equally important is the fact that climatic deterioration at the onset of the Younger Dryas was not associated with any major shift in material culture, the onset of late Natufian (final Epipalaeolithic) occurring before this around 13.5±0.2 ka BP (Henry, 2013). This suggests that while rapid climatic amelioration was associated with cultural innovation, confidence and risk-taking, climatic adversity prompted more conservative behaviours, and maintenance of established strategies that were already tried and tested. There are parallels here with Rosen and Rivera-Collazo's (2012) use of adaptive cycles to explain human responses to climate change during the Late Pleistocene/Holocene transition in the Levant. They argued, for example, that the Younger Dryas prompted greater societal resilience and use of low-risk resources in the face of colder, drier climatic conditions. By contrast, in the succeeding PPNA, the improved climate encouraged environmental opportunism and investment in high-risk but high-yield cultivation of morphologically-wild cereal grasses.

Rather than becoming mired in the difficulties of testing precise synchronism between changes in climate and human culture, we have aggregated all archaeological ^{14}C dates, regardless of cultural period, as a proxy for past population trends, as described in section 4. While these data should not be over-interpreted, especially when numbers of sites/dates are low, it is clear that different regions of southwest Asia showed different demographic trajectories through time (Fig. 8); in fact some regions had opposing rather than similar patterns, for example the northern Levant versus south-central Anatolia during the Younger Dryas and the beginning of the Holocene. There is no compelling evidence that some parts of the eastern Mediterranean region experienced fundamentally different climatic trends during the Late Pleistocene-early Holocene transition (e.g. with one area warming while another cooled). Instead, similar climatic trajectories had contrasting environmental or demographic consequences in different regions. During cold-dry time intervals (e.g. Younger Dryas) climatically-favoured regions acted as refugia for plant and animal resources and human populations. By contrast, most upland and interior regions of southwest Asia, such as central Anatolia, were dominated by low-biomass, resource-poor herb steppe at times of adverse climate, during which there is only limited evidence of human occupation (Figure 8).

In order to explore further the spatial implications of fluctuations in climate during the Last Glacial-Interglacial transition, we have created a series of mapped scenarios for different time intervals in the past. This analysis draws on the CRU TS3.10 0.5° gridded observations dataset (Harris et al., 2014;

https://crudata.uea.ac.uk/cru/data/hrg/), from which we have used mean values of mean monthly precipitation (MMP), mean annual temperature (MAT) and mean winter temperature (MTw, November to February) for the 1900-1950 reference period. Past precipitation and temperature in the eastern Mediterranean have been compiled for the Heinrich 1 (H1) event, the Bølling-Allerød interstadial, the Younger Dryas stadial, and the early Holocene. Temperature estimates derive principally from alkenone-based SSTs (table S5), as summarised in Almogi-Labin et al. (2009, fig. 7). These are probably minimum estimates for changes in air temperature, especially for winter and in interior land areas, where temperature depression is likely to have been greater than at the coast during the late Pleistocene. Estimates of past precipitation derive from stable isotope data at Soreq cave and Eski Acıgöl, using climatic calibration and isotope mass-balance modelling (summarised in Jones et al., 2007). These changes were applied uniformly across the whole region (i.e. the same drop/rise in temperature and the same % change in precipitation). Our analysis takes no account of changes in seasonality, although GCM experiments imply that the present-day summer drought, typical of Mediterranean-type climates, was much less prevalent in late Pleistocene times (see Wright, 1993, Fig. 5).

Notwithstanding these limitations and assumptions, the mapped scenarios shown in figure 9 clearly highlight that the same changes in climate had different consequences across the eastern Mediterranean region. Figure S10a and S10b show, respectively, MMP and MTw, while figure 9 combines the two climate parameters, using threshold values of -2°C (MPw) and 20 mm (MMP). Although arbitrary, this broadly corresponds to the modern agro-climatic limit for non-irrigated crop cultivation, and approximates to the climate space within which cereal domestication could have taken place. For Glacial (H1) times, the eastern Mediterranean *œcumene* was greatly reduced in extent, especially for interior Anatolia and northwest Iran; in contrast, the area of favourable climate in the southern Levant remained similar to that today. The eastern arm of the Fertile Crescent in Upper Mesopotamia is still identifiable under this scenario, but under climatic conditions any colder or drier than those used here, the east-west spatial connectivity along the Fertile Crescent would have become fragmented into isolated refugia (e.g. along river valleys). For the Bølling-Allerød interstadial scenario, the climatically-favourable land area more than doubled in extent, especially in areas such as the northern Levant/upper Mesopotamia and central Anatolia, although still with weak spatial connectivity between these two regions. It should be noted that there are divergences in climatic reconstruction for this time interval, with some reconstructions showing precipitation values above those at present (as used here) but others having values similar to today's. Thus the mapped area shown in figure 9 may be an over-estimate of the true *œcumene.* During the Younger Dryas reversal there was, unsurprisingly, a contraction in the favoured climate space, primarily involving inner Anatolia, whereas – significantly - continuity was maintained across the whole of the Fertile Crescent. This is consistent with the evidence for increasing population in the northern Levant throughout the Younger Dryas. Finally, in the early Holocene scenario, the climatic *œcumene* expanded to beyond its modern limits, including parts of the Syrian desert and almost all of Anatolia except the eastern

highlands. In climatic terms, there would have been strong spatial connectivity across the whole of southwest Asia other than the southern arid zone at this time.

It should be stressed that the maps shown in figure 9 represent scenarios of average climatic conditions that would have varied from year to year, and decade to decade. Little is currently known about whether inter-annual climate variability was different in the past from the modern instrumental period. What the scenarios suggest, however, is 1) temporal continuity of "favourable" climatic conditions in the southern Levant between glacial times and the early Holocene, 2) favourable climatic continuity from the Bølling-Allerød interstadial through the Younger Dryas in Upper Mesopotamia but 3) not in south central Anatolia, where winters became once again severe and moisture balance deficient during Younger Dryas times.

6. Conclusion

Neolithic agriculture in Southwest Asia has its origins during the preceding Epipalaeolithic cultures, coinciding with major changes in climate and vegetation, and following a long period of population increase. Pollen and charcoal evidence shows that there was an overall increase in woodland and grassland habitats and their associated plant and animal resources during the glacial-interglacial transition. Some of those environmental changes were of a speed and amplitude unprecedented in the last 20,000 years. Periods of rapid warming and wetting-up of the climate followed by climatic reversals prompted a range of human adaptive responses, including some that - with hindsight – we might view as evolutionary 'false starts' and dead ends, but others that eventually led to domestication of selected plants and animals (Fuller et al., 2013). Comparison of climatic and archeological data sets shows that in some areas, abrupt warming transitions at ~14.5 and 11.7 ka BP may have acted as pacemakers for rapid population increase, coinciding with the start of the Natufian and Pre-Pottery Neolithic cultures, respectively. However in other regions, such as central Anatolia, there is no clear synchronism evident between periods of rapid climatic amelioration and demographic trends. Although there is increasing evidence of human occupation of the Anatolian plateau during the Late Glacial interstadial and again early in the Holocene (Baird et al., 2013), the main rise in population and adoption of domesticates does not appear to have occurred here until after ~10.5 ka BP, i.e. more than a millennium after the shift in climate at the start of the Holocene.

Temporal synchroneity does not mean that climatic changes had the same environmental or societal consequences in different regions. During cold-dry time intervals (e.g. H1), favoured regions, such as the Levant, acted as refugia for plant and animal resources and human population. By contrast, most upland and interior regions were characterised by low-biomass resource-poor herb steppe at these times, and there is only limited evidence of human occupation of the Anatolian and Iranian plateaux. On the other hand, climate reconstructions suggest that interior regions below ~850 masl (e.g. northern Levant, Upper Mesopotamia, Zagros foothills) maintained conditions that were more

favourable for human occupation during the Younger Dryas stadial. This, in turn, would have allowed continuity of settlement here between the Late Glacial interstadial and the early Holocene. This is in good accord with ^{14}C PDF data which indicate a continued growth of population in the northern Levant and Upper Mesopotamia between ~13 and 11.3 ka BP. Unlike central Anatolia, there is no evidence of a demographic decline in the northern part of the Fertile Crescent coinciding with the Younger Dryas climatic reversal. Indeed, the northern Levant evidence, in particular, shows population growth continuing throughout the period; the peak here at the beginning of the Holocene is the culmination of a long-term trend, supporting long-standing arguments that increased sedentism and plant exploitation led to population growth. While early cultivation enabled further increase, it rapidly reached a limit, indicated by the flattening off in the population curve, and coinciding with the remarkable ritual and symbolic PPNA developments that are now familiar. This implies that in addition to demographic trends prompted by changes in the natural environment, some periods of regional population growth and decline in Southwest Asia during the early Holocene may have followed the kind of auto-cyclic "boom and bust" pattern seen in the primary Neolithic cultures of central and northwestern Europe (Shennan et al., 2013). Contrasting human responses to favourable climatic changes may have been set by antecedent conditions during preceding periods of climatic adversity. In areas where socio-ecological continuity was maintained through the Younger Dryas, such as the northern Levant, human communities and population levels clearly profited from the opportunities offered by the subsequent amelioration of climate and resources. By contrast, in areas where there was a climatically-driven discontinuity in settlement during Younger Dryas times (e.g. above ~850 masl), populations reacted more slowly to the new opportunities provided by the interglacial world. The consequences of climate change were not equal between regions or human communities in the past, just as they will not be in the future.

ACKNOWLEDGEMENTS

We are grateful for assistance, data and/or comments from Miryam Bar-Matthews, Hai Cheng, Warren Eastwood, Dominik Fleitmann, Lucia Wick, Rachid Cheddadi, Henk Woldring, Alexander Kabelindde, Fayrouz Ibrahim, two anonymous reviewers, European Pollen Database providers and EPD manager Michelle Leydet, and the Plymouth University Cartographic Unit, with special thanks to Shaun Lewin and Jamie Quinn.

This paper is dedicated to the memory of Herb Wright (1917-2015), who made seminal and pioneering studies of environmental change and agricultural origins in southwest Asia.

List of figures and tables

Supplementary information

Figure S10: Mapped climate scenarios for different time periods during the Last Glacial-Interglacial Transition

a) Mean annual and winter temperature
b) Mean annual precipitation

Table S1: Stable isotope records used in this study

Table S2: Pollen sites used in this study

Table S3: Changing proportions of woody plants by site and time period from archaeological charcoals

Table S4: Charcoal data by time period and region used for figure 5

Table S5: Palaeo-temperature and palaeo-precipitation estimates used for climate scenario modelling

References

Almogi-Labin, A., M. Bar-Matthews, D. Shriki, E. Kolosovsky, M. Paterne, B. Schilman, A. Ayalon, Z. Aizenshtat and A. Matthews 2009. Climatic variability during the last ~90 ka of the southern and northern Levantine basin as evident from marine records and speleothems. Quaternary Science Reviews 28, 2882-2896.

Asouti, E. and Austin, P. 2005. Reconstructing woodland vegetation and its exploitation by past societies, based on the analysis and interpretation of archaeological wood charcoal macro-remains. Environmental Archaeology 10, 1-18.

Asouti, E. and Fuller, D.Q., 2012. From foraging to farming in the southern Levant: The development of Epipalaeolithic and Pre-Pottery Neolithic plant management strategies. Vegetation History and Archaeobotany 21, 149-162.

Asouti E and Kabukcu C. 2014. Holocene semi-arid oak woodlands in the Irano-Anatolian region of Southwest Asia: natural or anthropogenic? Quaternary Science Reviews 90, 158–182.

Asouti, E., Kabukcu, C., White, C.E., Kuijt, I., Finlayson, B. and Makarewicz, C., 2015. Early Holocene woodland vegetation and human impacts in the arid zone of the southern Levant. The Holocene 25, 1565-1580

Bahr, A., Arz, H.W., Lamy, F., Wefer, G., 2006. Late glacial to Holocene paleoenvironmental evolution of the Black Sea, reconstructed with stable oxygen isotope records obtained on ostracod shells. Earth Planet. Sci. Lett. 241, 863-875.

Baird, D., Asouti, E., Astruc, L., Baysal, A., Baysal, E., Carruthers, D., Fairbairn, A., Kabukcu, C., et al., 2013. Juniper smoke, skulls and wolves' tails. The Epipalaeolithic of the Anatolian plateau in its SW Asian context; insights from Pınarbaşı. Levant 45, 175-209.

Baird, D., Fairbairn, A., Martin, L. and Middleton, C. 2012. The Boncuklu Project; the origins of sedentism, cultivation and herding in central Anatolia. In M. Özdoğan & N. Başgelen (eds), The Neolithic in Turkey: New Excavations and New Research. Istanbul: Arkeoloji ve Sanat Taslikliogl u, pp. 219-244.

Bar-Matthews, M., Ayalon, A. and Kaufman, A. 1997. Late Quaternary paleoclimate in the eastern Mediterranean region from stable isotope analysis of speleothems at Soreq Cave, Israel. Quaternary Research 47, 155-68.

Bar-Yosef, O., 2017. Facing climatic hazards: Paleolithic foragers and Neolithic farmers. Quaternary International 428 (B), 64-72

Barker, G. (2006) The Agricultural Revolution: Why Did Foragers Become Farmers? Oxford: Oxford University Press.

Bartov, Y., Goldstein, S.L., Stein, M., Enzel, Y., 2003. Catastrophic arid episodes in the Eastern Mediterranean linked with the North Atlantic Heinrich events. Geology 31, 439–442.

Baruch, U. and Bottema, S. 1991. Palynological evidence for climatic changes in the Levant ca. 17000-9000 B.P., in O.Bar-Yosef and F.R.Valla (eds) The Natufian

culture in the Levant. Ann Arbor, Michigan, International Monographs in Prehistory, pp.11-20

Baruch U, Bottema S. 1999. A new pollen diagram from Lake Hula: vegetational, climatic and anthropogenic implications. In Ancient Lakes: Their Cultural and Biological Diversity, Kawanabe H, Coulter GW, Roosevelt AC (eds), Kenobi Productions: Ghent, Belgium; pp. 75– 86.

Baruch, U. and Goring-Morris. A.N. 1997. The arboreal vegetation of the central Negev highlands, Israel, at the end of the Pleistocene: Evidence from archaeological charred wood remains. Veg. Hist. Archaeobot. 6, 249–259.

Berger, J.F., Lespez, L., Kuzucuoğlu, C., Glais, A., Hourani, F., Barra, A. and Guilaine, J. 2016. Interactions between climate change and human activities during the early to mid-Holocene in the eastern Mediterranean basins. Climate of the Past, 12, 1847-1877.

Blockley, S.P.E. and R. Pinhasi 2011. A revised chronology for the adoption of agriculture in the Southern Levant and the role of Lateglacial climatic change, Quaternary Science Reviews 30, 98-108.

Bocquet-Appel, J. P. 2002. Paleoanthropological traces of a Neolithic demographic transition. Current Anthropology 43, 637–647.

Böhner, U. and D. Schyle 2002-2006. Radiocarbon CONTEXT database, (doi:10.1594/GFZ.CONTEXT.Ed1)

Borrell, F., Junno, A. and Barceló, J.A. 2015. Synchronous Environmental and Cultural Change in the Emergence of Agricultural Economies 10,000 Years Ago in the Levant. PLoS ONE 10.8: e0134810 (doi:10.1371/journal.pone.0134810)

Bottema, S. 1986. A late Quaternary pollen diagram from Lake Urmia (northwestern Iran). Review of Palaeobotany and Palynology 47, 241–261.

Bottema, S., and W. van Zeist. 1981. Palynological evidence for the climatic history of the near East: 50,000-6000 BP, In Préhistoire du Levant. Colloques Internationaux du CNRS, 598. Editions CNRS, pp. 111-132.

Bottema, S. and Woldring, H. 1984. Late Quaternary vegetation and climate of southwestern Turkey, Part II. Palaeohistoria 26, 123–149.

Bottema S. 1995. The Younger Dryas in the eastern Mediterranean. Quaternary Science Reviews. 14, 883-91.

Brooks, C.E.P. 1926. Climate through the ages. London, Earnest Benn

Butzer, K.W. 1958. Quaternary stratigraphy and climate in the Near East. Bonner Geogr. Abh. Heft 24, 157 pp.

Cheddadi, R. and Khater, C. 2016. Climate change since the last glacial period in Lebanon and the persistence of Mediterranean species. Quaternary Science Reviews 150, 146-157.

Cheng, H., Sinha, A., Verheyden, S., Nader, F.H., Li, X.L., Zhang, P.Z., Yin, J.J., Yi, L., Peng, Y.B., Rao, Z.G., Ning, Y.F. and Edwards, R.L. 2015. The climate variability in northern Levant over the past 20,000 years. Geophysical Research Letters 10.1002/2015GL065397

Childe, V.G. 1928. The Most Ancient East. Kegan Paul, London

Colledge, S. and Conolly, J. 2010. Reassessing the evidence for the cultivation of wild crops during the Younger Dryas at Tell Abu Hureyra, Syria. Environmental Archaeology 15. 124-38.

Colledge, S., Connolly, J. and Shennan, S. 2004. Archaeobotanical evidence for the spread of farming in the Eastern Mediterranean, Current Anthropology 45, S35-S58.

Conolly, J., Colledge, S., Dobney, K., Vigne, J.-D., Peters, J., Stopp, B., Manning, K. and Shennan, S. 2011. Meta-analysis of zooarchaeological data from SW Asia and SE Europe provides insight into the origins and spread of animal husbandry. Journal of Archaeological Science 38, 538-545

Cowgill, U. M. 1969. The waters of Merom: a study of Lake Huleh I. Introduction and the general stratigraphy of a 54 m core. Archiv für Hydrobiologie 66, 249-72.

Crema, E. R., Habu, J., Kobayashi, K. and Madella, M. 2016. Summed Probability Distribution of ^{14}C Dates Suggests Regional Divergences in the Population Dynamics of the Jomon Period in Eastern Japan. PLOS ONE 11: e0154809 (doi: 10.1371/journal.pone.0154809)

Dean, J.R., Jones, M.D., Leng, M.J., Noble, S.R., Metcalfe, S.E., Sloane, H.J, Sahya, D., Eastwood, W.J. and Roberts, C.N. 2015. Eastern Mediterranean hydroclimate over the late glacial and Holocene, reconstructed from the sediments of Nar lake, central Turkey, using stable isotopes and carbonate mineralogy. Quaternary Science Reviews 124, 162–174.

Develle, A.L., Herreros, J., Vidal, L., Sursock, A. and Gasse, F., 2010. Controlling factors on a paleo-lake oxygen isotope record (Yammoûneh, Lebanon) since the Last Glacial Maximum. Quaternary Science Reviews 29, 865-886.

Djamali, M., Akhani, H., Andrieu-Ponel, V., Braconnot, P., Brewer, S., de Beaulieu, J-L., Fleitmann, D., Fleury, J., Gasse, F., Guibal, F., Jackson, S.T., Lézine, A-M., Médail, F., Ponel, F., Roberts, N. and Stevens, L. 2010. Indian Summer Monsoon variations could have affected the early Holocene woodland expansion in the Near East. The Holocene 20, 813-20

Emeis, K.C., U. Struck, H.M. Schulz, R. Rosenberg, S. Bernasconi, H. Erlenkeuser, T. Sakamoto and F. Martinez-Ruiz 2000. Temperature and salinity variations of Mediterranean Sea surface waters over the last 16,000 years from records of planktonic stable oxygen isotopes and alkenone unsaturation ratios. Palaeogeog. Palaeoclim. Palaeoecol. 158, 259–280.

Enzel, Y., Amit, R., Dayan, U., Crouvi, O., Kahana, R., Ziv, B. and Sharon, D. 2008. The climatic and physiographic controls of the eastern Mediterranean over the late Pleistocene climates in the southern Levant and its neighboring deserts. Global and Planetary Change 60, 165–192.

Essallami L., Sicre, M.A., Kallel, N., Labeyrie, L., Siani, G., 2007. Hydrological changes in the Mediterranean Sea over the last 30,000 years. Geochemistry, Geophysics, Geosystems 8, Q07002, doi:10.1029/2007GC001587.

Flannery, K.V. 1969. Origins and ecological effects of early domestication in Iran and the Near East. In: P. Ucko and G. Dimbleby (eds), *The domestication and exploitation of plants and animals*, London: Duckworth, pp. 73-100.

Flohr, P., Fleitmann, D., Matthews, R., Matthews, W. and S. Black 2016. Evidence of resilience to past climate change in Southwest Asia: Early farming communities and the 9.2 and 8.2 ka events, Quaternary Science Reviews 136, 23-39.

Frumkin, A., Ford, D.C. and Schwarcz, H.P. 1999. Continental oxygen isotopic record of the last 170,000 years in Jerusalem. Quaternary Research 51, 317-27.

Fuller, D.Q., Willcox, G. and Allaby, R.G. 2012. Early agricultural pathways: moving outside the 'core area' hypothesis in Southwest Asia. Journal of Experimental Botany 63, 617–633.

Gasse, F., Vidal, L., Van Campo, E., Demory, F., Develle, A.L., Tachikawa, K., Elias, A., Bard, E., Garcia, M., Sonzogni, C. and Thouveny, N., 2015. Hydroclimatic changes in northern Levant over the past 400,000 years. Quaternary Science Reviews 111, 1-8.

Göktürk, O.M., D. Fleitmann, S. Badertscher, H. Cheng, R.L. Edwards and O. Tüysüz 2011. Climate on the Southern Black Sea coast during the Holocene, Quaternary Science Reviews 30, 2433–2445.

Goring-Morris, A.N. and Belfer-Cohen, A., 2008. A roof over one's head: Developments in Near Eastern residential architecture across the Epipalaeolithic–Neolithic transition. In: J. P. Boquet-Appel and O. Bar-Yosef (eds), The Neolithic demographic transition and its consequences. Dordrecht: Springer Netherlands, pp. 239-286.

Goring-Morris, N. and A. Belfer-Cohen 2010. 'Great Expectations', or the inevitable collapse of the early Neolithic in the Near East. In M. Bandy and J. Fox (eds), Becoming Villagers: Comparing Village Societies, Tucson: University of Arizona Press, pp. 62-77.

Goudie, A. 1973. The concept of post-glacial progressive desiccation. School of Geography, University of Oxford, Discussion Paper.

Grant, K.M., Rohling, E.J., Bar-Matthews, M., Ayalon, A., Medina-Elizalde, M., Bronk Ramsey, C., Satow, C. and Roberts, A.P. 2012. Rapid coupling between ice volume and polar temperature over the past 150,000 years. Nature 491, 744-747.

Grootes, P.M., and M. Stuiver. 1997. Oxygen 18/16 variability in Greenland snow and ice with 10^3 to 10^5-year time resolution. Journal of Geophysical Research 102, 26455-70.

Guerrero, E., Naji, S., Bocquet-Appel, J.-P., 2008. The signal of the Neolithic demographic transition in the Levant. In: Bocquet-Appel, J.-P., Bar-Yosef, O. (eds), The Neolithic Demographic Transition and Its Consequences. Springer ScienceþBusiness Media B.V., pp. 57-80.

Hajar, L., Haïdar-Boustani, M., Khater, C., et al. 2010. Environmental changes in Lebanon during the Holocene: Man vs. climate impacts. Journal of Arid Environments 74, 746–755.

Hajar, L., Khater, C. and Cheddadi, R. 2008. Vegetation changes during the late Pleistocene and Holocene in Lebanon: a pollen record from the Bekaa Valley. The Holocene 18, 1089–1099.

Harris, D.R. 1998. The origins of agriculture in southwest Asia. Review of Archaeology 19, 5-11.

Harris, I., Jones, P.D., Osborn, T.J. and Lister, D.H. 2014. Updated high-resolution grids of monthly climatic observations – the CRU TS3.10 Dataset. International Journal of Climatology 34, 623–642 [plus correction to the above paper: Revised Appendix 3 (CLD)]

Henry, D.O. 2013. The Natufian and the Younger Dryas. In O. Bar-Yosef and F.R. Valla (eds) Natufian Foragers in the Levant. International Monographs in Prehistory 19, Ann Arbor, Michigan, pp. 584-610.

Heun, M., Schäfer-Pregl, R., Klawan, D., Castagna, R., Accerbi, M., Borghi, B. and Salamini, F. 1997. Site of einkorn wheat domestication identified by DNA fingerprinting. Science 278, 1312-1314.

Hillman, G. 1996. Late Pleistocene changes in wild plant-foods available to hunter-gatherers of the northern Fertile Crescent: possible preludes to cereal cultivation, in D.R.Harris (ed.) The origins and spread of agriculture and pastoralism in Eurasia. London: UCL Press, pp.159-203.

Hogg, A., Southon, J., Turney, C., Palmer, J., Ramsey, C.B., Fenwick, P., Boswijk, G., Büntgen, U., Friedrich, M., Helle, G., Hughen, K., Jones, R., Kromer, B., Noronha, A., Reinig, F., Reynard, L., Staff, R. and Wacker, L. 2016. Decadally Resolved Lateglacial Radiocarbon Evidence from New Zealand Kauri. Radiocarbon 58, 709–733.

Hutchinson, G.E. and Cowgill, U.M. 1963. Chemical examination of a core from Lake Zeribar, Iran. Science 140, 67-69

Jones, M.D., Roberts, C.N. and Leng, M.J. 2007. Quantifying climatic change through the LGIT based on lake isotope palaeohydrology from central Turkey. Quaternary Research 67, 463-473.

Kolodny, Y., Stein, M., Machlus, M. 2005. Sea-rain-lake relation in the Last Glacial East Mediterranean revealed by $\delta^{18}O$-$\delta^{13}C$ in Lake Lisan aragonites. Geochim. Cosmochim. Acta 69, 4045-60.

Kuijt, I., 2000. People and space in early agricultural villages: exploring daily lives, community size, and architecture in the late pre-pottery Neolithic. Journal of Anthropological Archaeology 19, 75-102.

Kuijt, I., 2008. Demography and storage systems during the southern Levantine Neolithic demographic transition. In: J. P. Boquet-Appel and O. Bar-Yosef (eds), The Neolithic demographic transition and its consequences. Dordrecht: Springer Netherlands, pp. 287-313.

Kwiecien, O., Stockhecke, M., Pickarski, N., Heumann, G., Litt, T., Sturm, M., Anselmetti, F., Kipfer, R. and Haug, G.H., 2014. Dynamics of the last four glacial terminations recorded in Lake Van, Turkey. Quaternary Science Reviews 104, 42-52.

Lechterbeck, J., Edinborough, K., Kerig, T., Fyfe, R., Roberts, N. and Shennan, S., 2014. Is Neolithic land use correlated with demography? An evaluation of pollen-derived land cover and radiocarbon-inferred demographic change from Central Europe. The Holocene 24, 1297-1307.

Leng, M.J., Roberts, N., Reed, J.M. and Sloane, H.J. 1999. Late Quaternary palaeohydrology of the Konya Basin, Turkey based on isotope studies of modern hydrology and lacustrine carbonates. Journal of Paleolimnology 22, 187-204.

Litt T, Krastel S, Sturm M, Kipfer R, Örcen S, Heumann G, Franz SO, Ülgen UB, Niessen F. 2009. Lake Van Drilling Project 'PALEOVAN': results of a recent pre-site survey and perspectives. Quaternary Science Reviews 28, 1555–1567.

Lotter, A.F. 2003. Multi-proxy climatic reconstructions, in A. Mackay, R. Battarbee, J. Birks and F. Oldfield (eds) Global Change in the Holocene. London: Arnold, pp. 373-83.

Maedaa, O., Lucas, L., Silva, F., Tanno, K-I. and Fuller, D.Q. 2016. Narrowing the harvest: Increasing sickle investment and the rise of domesticated cereal agriculture in the Fertile Crescent, Quaternary Science Reviews 145, 226-237.

Maher, L.A., E.B. Banning and M. Chazan 2011. Oasis or Mirage? Assessing the Role of Abrupt Climate Change in the Prehistory of the Southern Levant. Cambridge Archaeological Journal 21, 1-29.

Makarewicz, C.A., 2012. The Younger Dryas and hunter-gatherer transitions to food production in the Near East. In: Erin, M. (ed.), Hunter Gatherer Behavior: Human Response During the Younger Dryas. Walnut Creek: Left Coast Press, pp. 195-230.

Meadows J. 2005. The Younger Dryas episode and the radiocarbon chronologies of the Lake Huleh and Ghab Valley pollen diagrams, Israel and Syria. The Holocene 15, 631–636.

Meltzer, D.J. and Bar-Yosef, O., 2012. Looking for the Younger Dryas. In: Erin, M. (ed.), Hunter Gatherer Behavior: Human Response During the Younger Dryas. Walnut Creek: Left Coast Press, pp. 249-267.

Mithen, S.J., Austin, P., Kennedy, A. et al. 2007. Neolithic woodland composition and exploitation in the Southern Levant: a comparison between archaeobotanical remains from WF16 and present day woodland at Hammam Adethni. Environmental Archaeology 12, 49–70.

Moore, A.M.T. and Hillman, G.C. 1992. The Pleistocene to Holocene transition and human economy in Southwest Asia: the impact of the Younger Dryas, American Antiquity 57, 482-494.

Nesbitt, M. 2002. When and where did domesticated cereals first occur in Southwest Asia? In R.T.J. Cappers and S.Bottema (eds) The dawn of farming in the Near East. Berlin (SENEPSE 6) ex oriente, pp. 113–132

Peake, H. and Fleure, H.J. 1927. The corridors of time. Volume III, Peasants and Potters. Oxford University Press.

Prendergast, A.L., Stevens, R.E., O'Connell, T.C., Hill, E.A., Hunt, C. and Barker, G.W., 2016. A late Pleistocene refugium in Mediterranean North Africa?

Palaeoenvironmental reconstruction from stable isotope analyses of land snail shells (Haua Fteah, Libya). Quaternary Science Reviews 139, 94-109.

Pumpelly, R., 1908. Ancient Anau and the Oasis-World. Explorations in Turkestan, Expedition of 1904. Prehistoric Civilizations of Anau, Origins, Growth, and Influence of Environment. Carnegie institution of Washington, Vol. 73, pp. 1-80.

Reed, C.A. and Braidwood, R.J. 1960. Toward a reconstruction of the environmental sequence of northeastern Iraq. In R.J. Braidwood and B. Howe (eds) Prehistoric investigations in Iraqi Kurdistan. Oriental Institute, Chicago publication 31, pp.163-174.

Riehl S., Zeidi M., and Conard N.J. 2013. Emergence of agriculture in the foothills of the Zagros mountains of Iran. Science 341, 65-57.

Riehl, S., Asouti, E., Karakaya, D., Starkovich, B.M., Zeidi, M., Conard, N.J. 2015. Resilience at the transition to agriculture: the long-term landscape and resource development at the aceramic Neolithic tell site of Chogha Golan (Iran). BioMed Research International, 2015, Article ID 532481.

Roberts, N. 2002 Did prehistoric landscape management retard the post-glacial spread of woodland in Southwest Asia? Antiquity 76, 1002-10.

Roberts, N., Allcock, S.L., Arnaud, F., Dean, J.R., Eastwood, W.J., Jones, M.D., Leng, M.J., Metcalfe, S.E., Malet, E., Woodbridge, J. and Yiğitbaşıoğlu, H. 2016. A tale of two lakes: a multi-proxy comparison of Late Glacial and Holocene environmental change in Cappadocia, Turkey. Journal of Quaternary Science 31, 348–362

Roberts, N., Black, S., Boyer, P., Eastwood, W.J., Griffiths, H., Leng, M., Parish, R., Reed, J., Twigg, D. and Yigitbasioglu, H. 1999. Chronology and Stratigraphy of Late Quaternary sediments in the Konya Basin, Turkey: results from the KOPAL project. Quaternary Science Reviews 18, 611-630.

Roberts, N., Eastwood, W.J., Kuzucuoğlu, C., Fiorentino, G. and Caracuta, V. 2011. Climatic, vegetation and cultural change in the eastern Mediterranean during the mid-Holocene environmental transition. The Holocene 21, 147-162.

Roberts, N., Jones, M.D., Benkaddour, A., Eastwood, W.J., Filippi, M.L., Frogley, M.R., Lamb, H.F., Leng, M.J., Reed, J.M., Stein, M., Stevens, L., Valero-Garcés, B. and Zanchetta, G.. 2008. Stable isotope records of Late Quaternary climate and hydrology from Mediterranean lakes: the ISOMED synthesis. Quaternary Science Reviews. 27, 2426–2441.

Roberts, N., Reed, J., Leng, M.J., Kuzucuoğlu, C., Fontugne, M., Bertaux, J., Woldring, H., Bottema, S., Black, S., Hunt, E. and Karabıyıkoğlu, M. 2001. The tempo of Holocene climatic change in the eastern Mediterranean region: new high-resolution crater-lake sediment data from central Turkey. The Holocene 11, 721-736.

Robinson, S.A., Black, S., Sellwood, B.W., Valdes, P.J. 2006. A review of paleoclimates and palaeoenvironments from the Levant and Eastern Mediterranean from 25,000 to 5,000 years BP: setting the environmental background for the evolution of human civilization. Quaternary Science Reviews 25, 1517–1541.

Rosen, A.M. and Rivera-Collazo, I. 2012. Climate change, adaptive cycles, and the persistence of foraging economies during the Late Pleistocene/Holocene transition in the Levant, Proceedings, National Academy of Sciences USA 109, 3640-45.

Rossignol-Strick, M. 1995. Sea-land correlation of pollen records in the eastern Mediterranean for the glacial-interglacial transition: Biostratigraphy versus radiometric time-scale. Quaternary Science Reviews 14, 893-915.

Rossignol-Strick, M. 1999. The Holocene climatic optimum and pollen records of sapropel 1 in the eastern Mediterranean, 9000-6000 BP. Quaternary Science Reviews 18, 515-530.

Sarıkaya, M.A., Zreda, M. and Çiner, A. 2009. Glaciations and paleoclimate of Mount Erciyes, central Turkey, since the Last Glacial Maximum, inferred from 36Cl cosmogenic dating and glacier modelling, Quaternary Science Reviews 28, 2326-2341.

Sarıkaya, M.A., Zreda, M., Çiner, A. and Zweck, C. 2008. Cold and wet Last Glacial Maximum on Mount Sandıras, SW Turkey, inferred from cosmogenic dating and glacier modelling. Quaternary Science Reviews 27, 769–780.

Shennan, S., Downey, S.S., Timpson, A., Edinborough, K., Colledge, S., Kerig, T., Manning, K. and Thomas, M.G. 2013. Regional population collapse followed initial agriculture booms in mid-Holocene Europe, Nature Communications 4 (doi: 10.1038/ncomms3486).

Stevens, L.R., Wright, H.E. Jr, and Ito, E. 2001. Proposed changes in seasonality of climate during the late-glacial and Holocene at Lake Zeribar, Iran. The Holocene 11, 747-756.

Stiner, M.C., Buitenhuis, H., Duru, G., Kuhn, S.L., Mentzer, S.M., Munro, N.D., Pöllath, N., Quade, J., Tsartsidou, G. and Özbaşaran, M. 2014. A forager–herder trade-off, from broad-spectrum hunting to sheep management at Aşıklı Höyük, Turkey. Proceedings of the National Academy of Sciences 111, 8404-8409.

Stockhecke, M., Timmermann, A., Kipfer, R., Haug, G.H., Kwiecien, O., Friedrich, T., Menviel, L., Litt, T., Pickarski, N. and Anselmetti, F.S., 2016. Millennial to orbital-scale variations of drought intensity in the Eastern Mediterranean. Quaternary Science Reviews 133, 77-95.

Timpson, A., Colledge, S., Crema, E., Edinborough, K., Kerig, T., Manning, K., Thomas, M.G. and Shennan, S. 2014. Reconstructing regional population fluctuations in the European Neolithic using radiocarbon dates: a new case-study using an improved method. Journal of Archaeological Science 52, 549-557.

Turner, R., Roberts, N., Eastwood, W.J., Jenkins, E. and Rosen, A. 2010. Fire, climate and the origins of agriculture: micro-charcoal records of biomass burning during the Last Glacial Interglacial Transition in Southwest Asia. Journal of Quaternary Science 25, 371–386.

Ünal-İmer, E., Shulmeister, J., Zhao, J.X., Uysal, I.T., Feng, Y.X., Nguyen, A.D. and Yüce, G., 2015. An 80 kyr-long continuous speleothem record from Dim Cave, SW Turkey with paleoclimatic implications for the Eastern Mediterranean. Scientific reports 5, p.13560.

Vaks, A., Bar-Matthews, M., Ayalon, A., Matthews, A., Frumkin, A., Dayan, U., Halicz, L., Almogi-Labin, A. and Schilman, B. 2006. Paleoclimate and location of the border between Mediterranean climate region and the Saharo-Arabian desert as revealed by speleothems from the northern Negev Desert, Israel. Earth and Planetary Science Letters 249, 384-99.

van Zeist, W. and Bottema, S. 1991. Late Quaternary vegetation of the Near East. Beihefte zum Tübinger Atlas des Vorderen Orients, Reihe A18, Dr L. Reichert Verlag, Wiesbaden, 156 pp.

van Zeist, W. and Wright, H.E. Jr. 1963. Preliminary pollen studies at Lake Zeribar, Zagros mountains, southwestern Iran. Science 140, 65-67.

Verheyden, S., Nader, F.H., Cheng, H.J., Edwards, L.R. and Swennen, R. 2008. Paleoclimate reconstruction in the Levant region from the geochemistry of a Holocene stalagmite from the Jeita cave, Lebanon. Quaternary Research 70, 368-81.

Walker, M., Johnsen, S., Rasmussen, S.O., Popp, T., Steffensen, J.-P., Gibbard, P., Hoek, W., Lowe, J., Andrews, J., Björck, S., Cwynar, L. C., Hughen, K., Kershaw, P., Kromer, B., Litt, T., Lowe, D. J., Nakagawa, T., Newnham, R., and Schwander, J. (2009) Formal definition and dating of the GSSP (Global Stratotype Section and Point) for the base of the Holocene using the Greenland NGRIP ice core, and selected auxiliary records. Journal of Quaternary Science 24, 3-17.

Weninger, B., Clare, L., Rohling, E., Bar-Yosef, O., Boehner, U., Budja, M., Bundschuh, M., Feurdean, A., Gebe, H.G., Joeris, O., Lindstaedter, J., Mayewski, P., Muehlenbruch, T., Reingruber, A., Rollefson, G., Schyle, D., Thissen, L., Todorova, H.and Zielhofer, C. 2009. The impact of rapid climate change on prehistoric societies during the Holocene in the Eastern Mediterranean. Documenta Praehistorica 36, 7-59 (doi:10.4312/dp.36.2).

Weninger, B., Clare, L., Jöris, O., Jung, R. and Edinborough, K. 2015. Quantum theory of radiocarbon calibration. World Archaeology 47, 543-566.

Wick L, Lemcke G and Sturm M. 2003. Evidence of Lateglacial and Holocene climatic change and human impact in eastern Anatolia: high-resolution pollen, charcoal, isotopic and geochemical records from laminated sediments of Lake Van, Turkey. The Holocene 13, 665–675.

Willcox, G. and Stordeur, D., 2012. Large-scale cereal processing before domestication during the tenth millennium cal BC in northern Syria. Antiquity 86, 99-114.

Willcox, G., Buxo, R. and Herveux, L. 2009. Late Pleistocene and early Holocene climate and the beginnings of cultivation in northern Syria. The Holocene 19, 151-158.

Woldring, H. and Bottema, S. 2003. The vegetation history of East-Central Anatolia in relation to Archaeology: the Eski Acıgöl pollen evidence compared with the near Eastern Environment. Palaeohistoria 43/44, 1–34.

Winterhalder, B. and Goland, C. 1993. On population, foraging efficiency, and plant domestication. Current Anthropology 34, 710-715.

Woodbridge, J., Fyfe, R.M., Roberts, N., Downey, S., Edinborough, K. and Shennan, S., 2014. The impact of the Neolithic agricultural transition in Britain: a comparison of pollen-based land-cover and archaeological ^{14}C date-inferred population change. Journal of Archaeological Science 51, 216-224.

Wright, H.E. Jr. 1962. Pleistocene glaciation in Kurdistan. Eiszeitalter und Gegenwart 12, 131-164.

Wright, H.E. Jr. 1968. The natural environment of early food production north of Mesopotamia. Science 161, 334-339.

Wright, H.E. Jr. 1976. Environmental setting for plant domestication in the Near East. Science 194, 385-389.

Wright, H.E. Jr. 1980. Climatic change and plant domestication in the Zagros mountains. Iran 18, 145-48.

Wright, H.E., Jr. 1993. Environmental determinism in Near Eastern Prehistory, Current Anthropology 34, 458-469.

Zeder, M. 2011. The Origins of Agriculture in the Near East, Current Anthropology 52, S221-S235.

Zeder, M.A. and Hesse, B. 2000. The Initial Domestication of Goats (Capra hircus) in the Zagros Mountains 10,000 Years Ago. Science 287, 2254-2257.

Zohary, D. and Hopf, M. 2001. Domestication of plants in the Old World. The origin and spread of cultivated plants in west Asia, Europe and the Nile valley. Oxford: Clarendon Press, 3rd ed.


Sofular
Eski Acıgöl
Aşıklı Höyük
Çatalhöyük
Akgöl
Lake Söğüt
Can Hasan
Dim
1
Lake Van
Çayönü
Hallan Çeme
Urmia
2
Jarmo
Lake Zeribar
Mureybit
Ghab
Abu Hureyra
3a
River Tigris
River Euphrates
Mediterranean Sea
Jeita
A / C / J
Tell Aswad
Ain Mallaha
Lake Huleh
Soreq
Jericho
3b
Wadi Faynan
Negev
N
0 km 400
Archaeological site
Cave sequence
Pollen core site
Probable extent of wild cereals at the end of the Pleistocene (after Hillman, 1996)

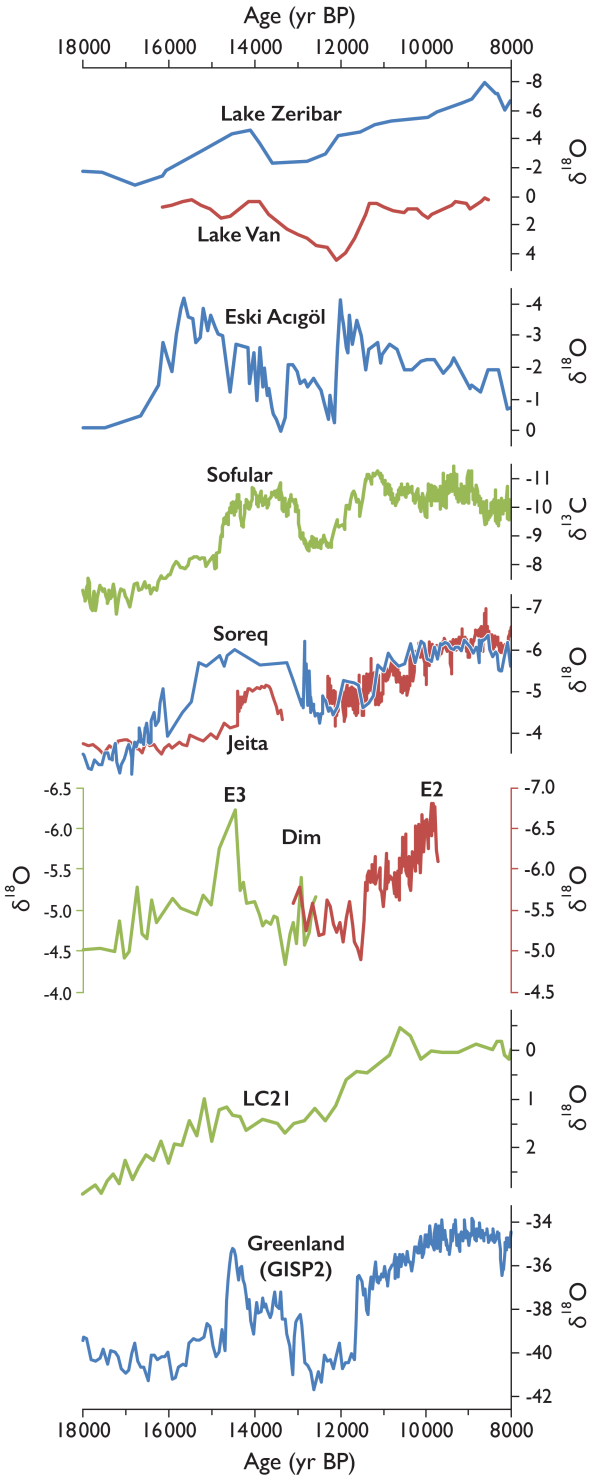
Age (yr BP)
18000
16000
14000
12000
10000
8000
Lake Zeribar
Lake Van
Eski Acıgöl
Sofular
Soreq
Jeita
E3
E2
Dim
LC21
Greenland
(GISP2)
δ18O
δ13C

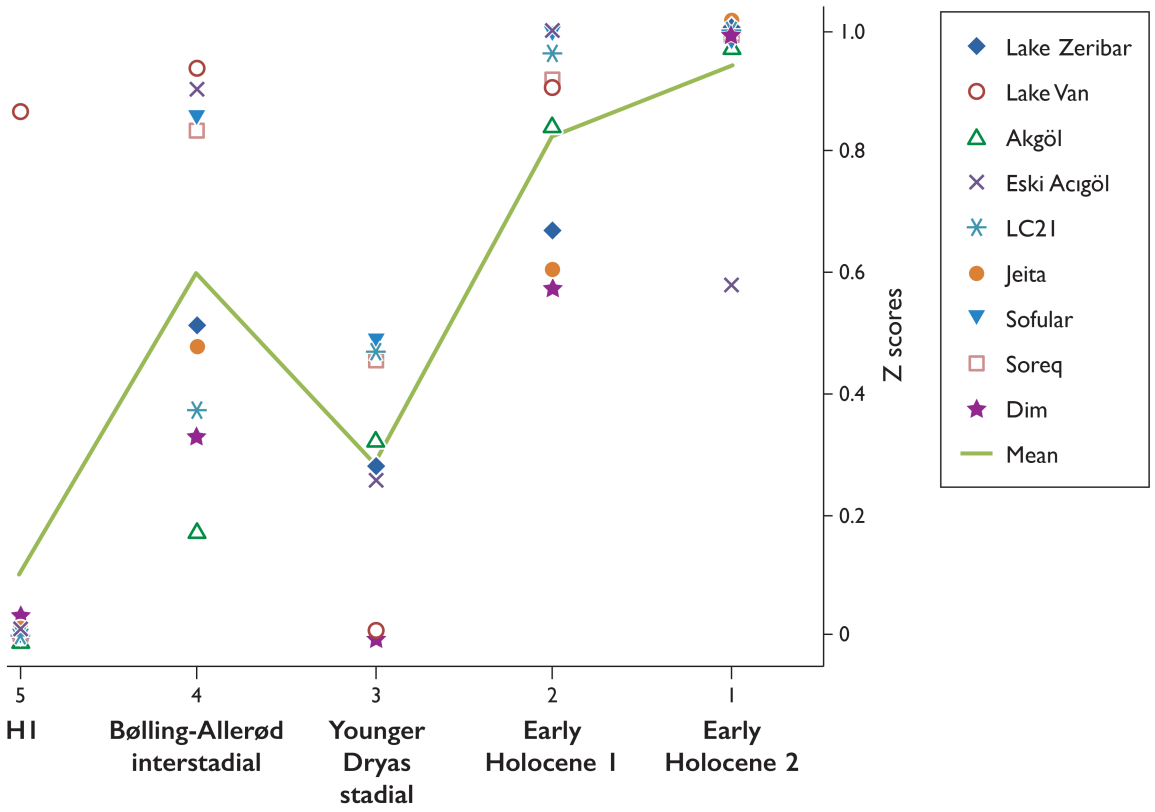
1.0
0.8
0.6
0.4
0.2
0
Z scores
5
4
3
2
1
H1
Bølling-Allerød interstadial
Younger Dryas stadial
Early Holocene 1
Early Holocene 2
Lake Zeribar
Lake Van
Akgöl
Eski Acıgöl
LC21
Jeita
Sofular
Soreq
Dim
Mean

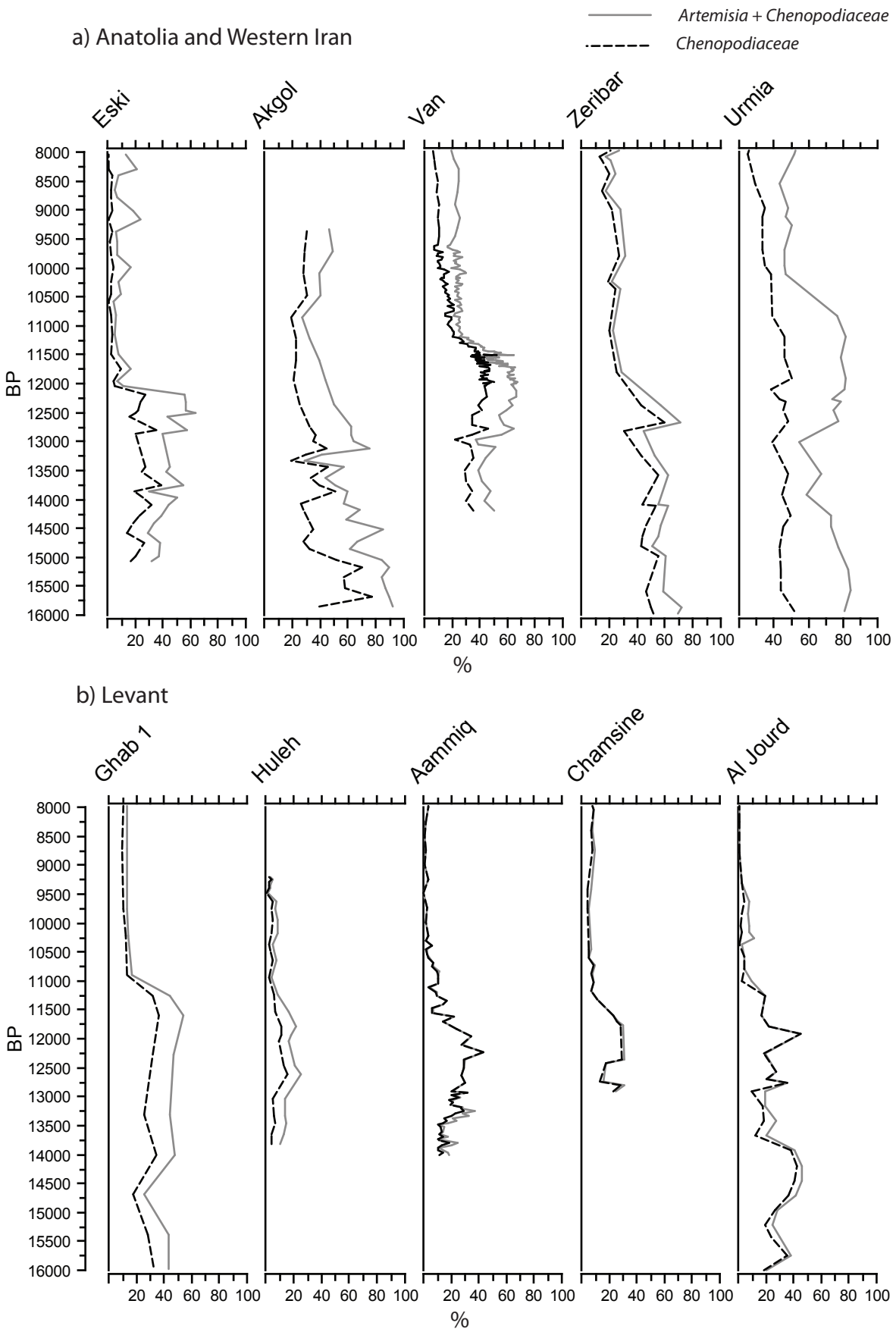
a) Anatolia and Western Iran
Artemisia + Chenopodiaceae
Chenopodiaceae
Eski
Akgol
Van
Zeribar
Urmia
BP
%
b) Levant
Ghab 1
Huleh
Aammiq
Chamsine
Al Jourd
BP
%

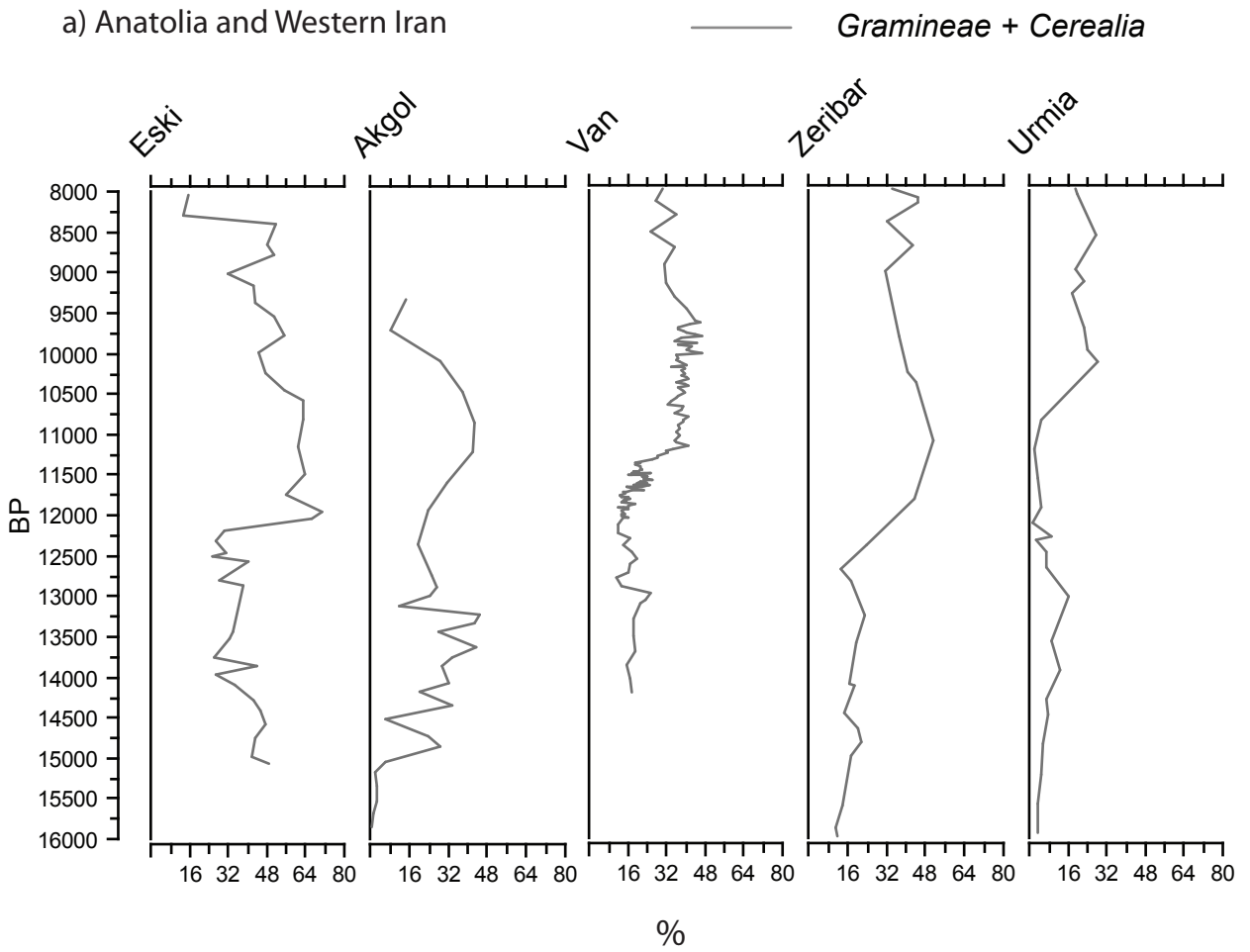
a) Anatolia and Western Iran
Gramineae + Cerealia
Eski
Akgol
Van
Zeribar
Urmia
BP
8000
8500
9000
9500
10000
10500
11000
11500
12000
12500
13000
13500
14000
14500
15000
15500
16000
16 32 48 64 80
%

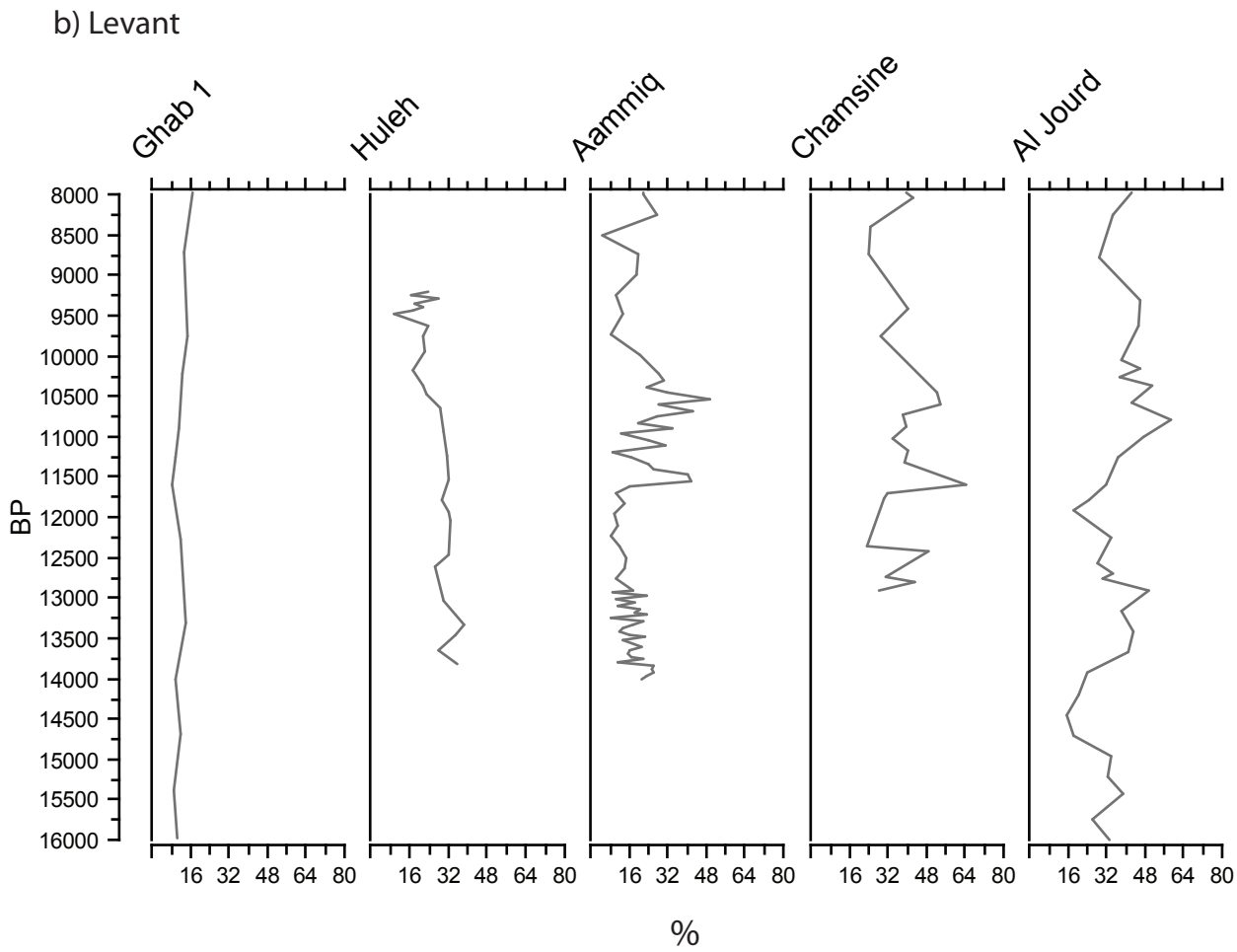
b) Levant
Ghab 1
Huleh
Aammiq
Chamsine
Al Jourd
BP
8000
8500
9000
9500
10000
10500
11000
11500
12000
12500
13000
13500
14000
14500
15000
15500
16000
16 32 48 64 80
%

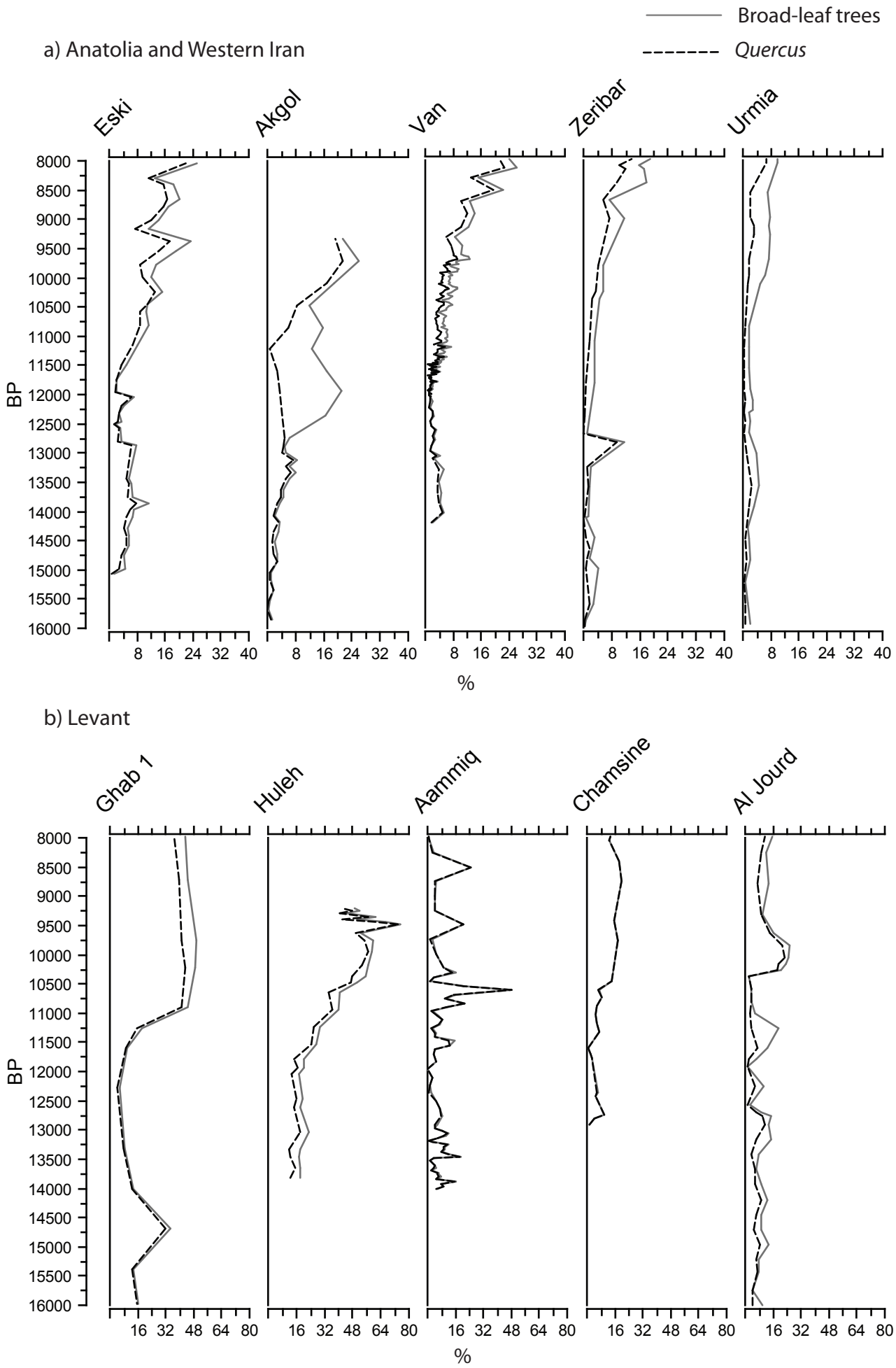
Broad-leaf trees
Quercus
a) Anatolia and Western Iran
Eski
Akgol
Van
Zeribar
Urmia
BP
8000
8500
9000
9500
10000
10500
11000
11500
12000
12500
13000
13500
14000
14500
15000
15500
16000
8 16 24 32 40
%
b) Levant
Ghab 1
Huleh
Aammiq
Chamsine
Al Jourd
16 32 48 64 80

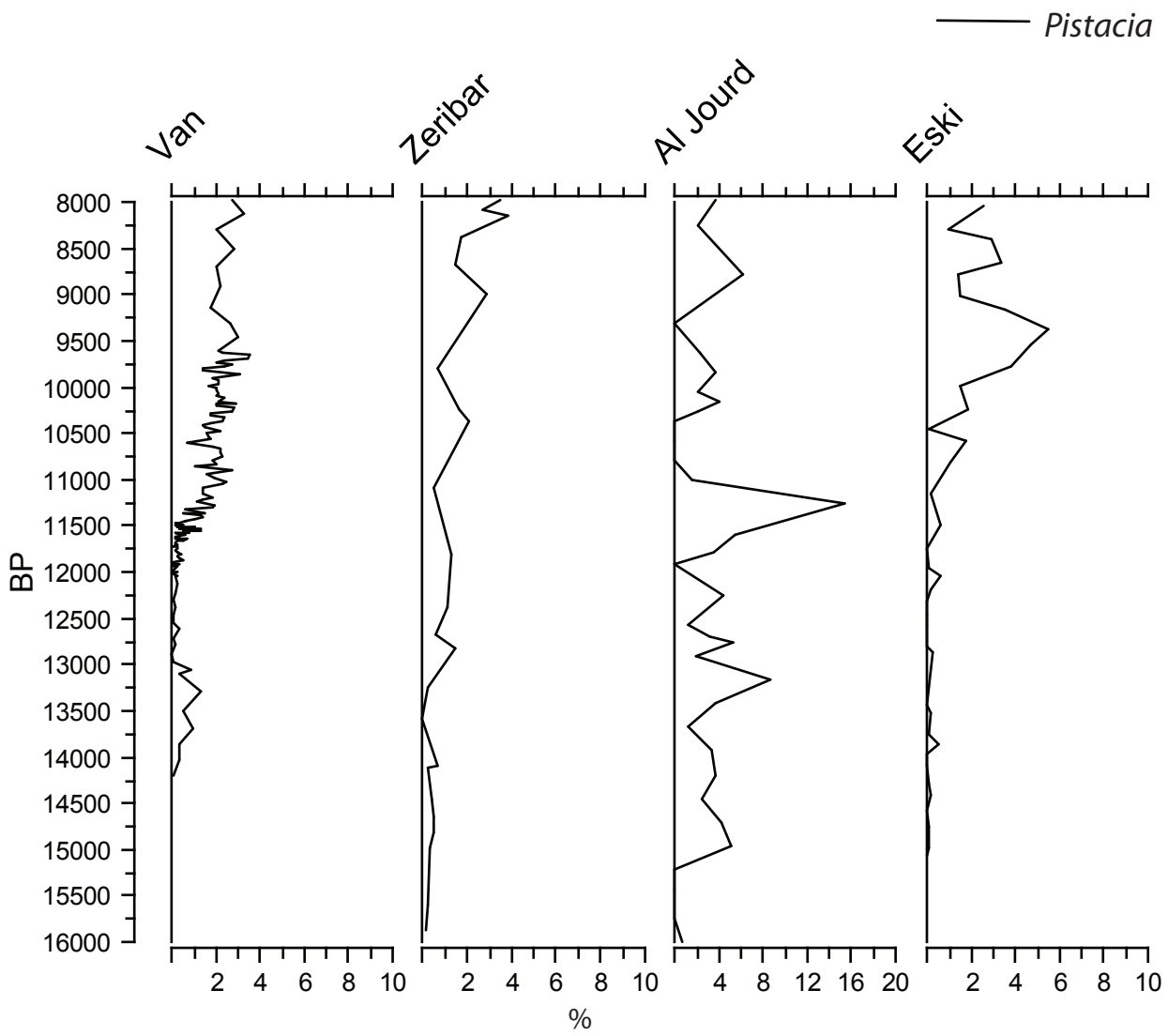
Pistacia
Van
Zeribar
Al Jourd
Eski
BP
8000
8500
9000
9500
10000
10500
11000
11500
12000
12500
13000
13500
14000
14500
15000
15500
16000
2 4 6 8 10
2 4 6 8 10
4 8 12 16 20
2 4 6 8 10
%

Climate phase	H1	B/A	YD	E Hol 1	E Hol 1
Archaeological period	"Kebaran"	Early Natufian	Late Natufian	PPNA-EPPNB	M-LPPNB
Southern Levant			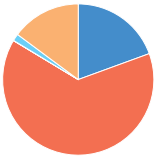	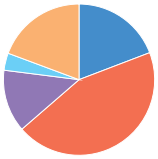	
South Central Anatolia		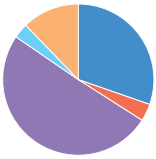		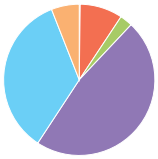	
SE Anatolia / N Iraq / W Iran				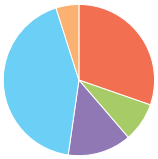	

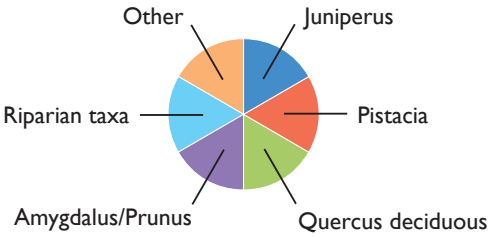

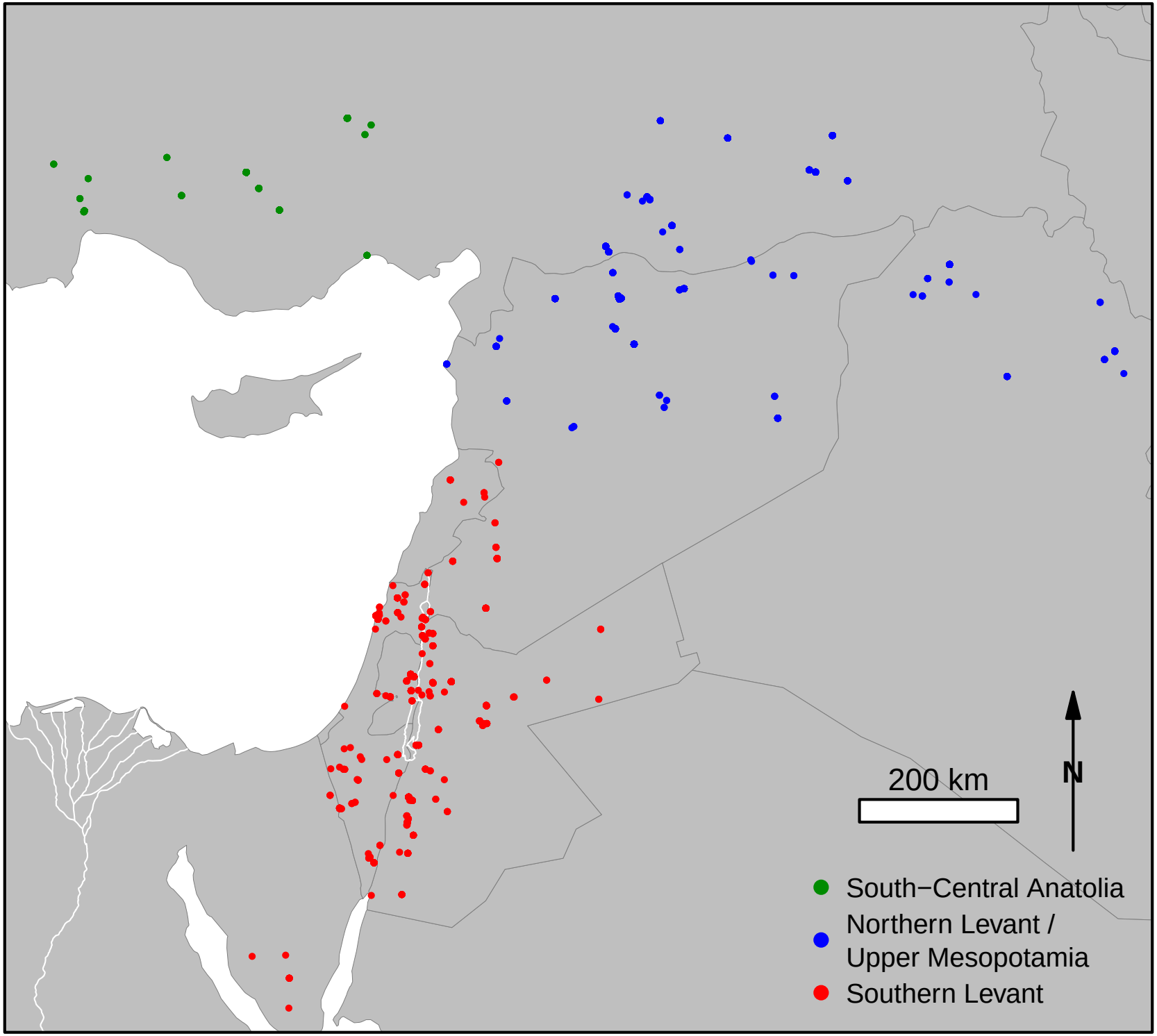
200 km
N
South−Central Anatolia
Northern Levant /
Upper Mesopotamia
Southern Levant

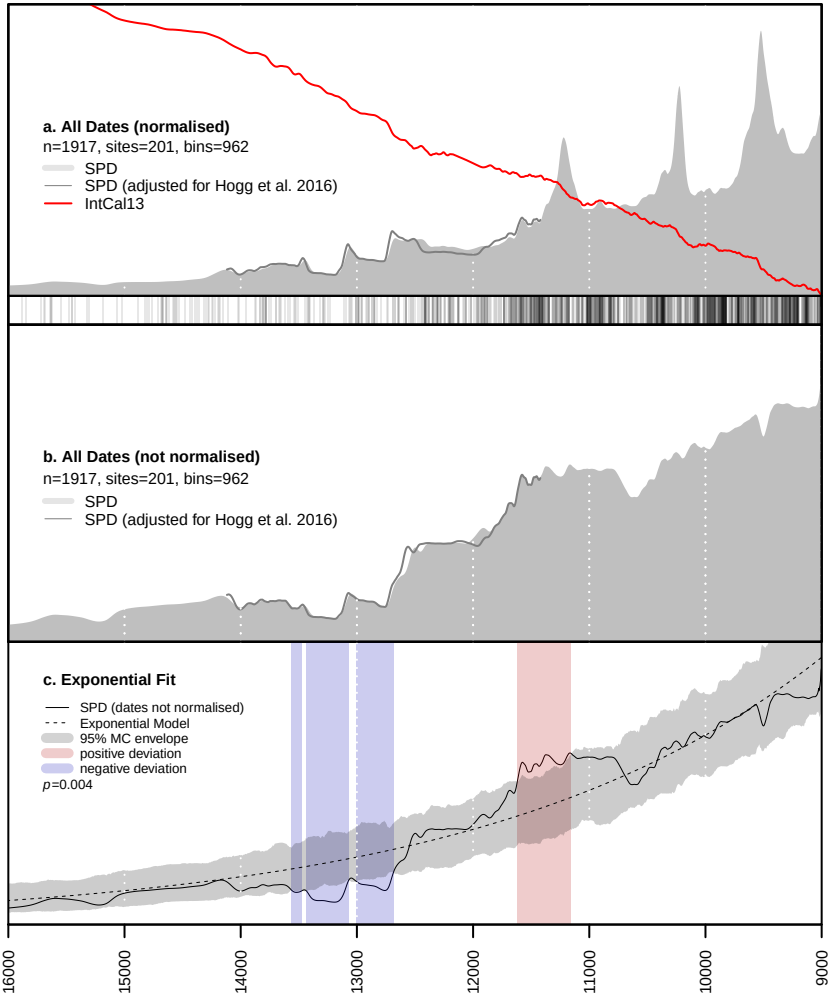
a. All Dates (normalised)
n=1917, sites=201, bins=962
SPD
SPD (adjusted for Hogg et al. 2016)
IntCal13
b. All Dates (not normalised)
n=1917, sites=201, bins=962
SPD
SPD (adjusted for Hogg et al. 2016)
c. Exponential Fit
SPD (dates not normalised)
Exponential Model
95% MC envelope
positive deviation
negative deviation
p=0.004
16000
15000
14000
13000
12000
11000
10000
9000

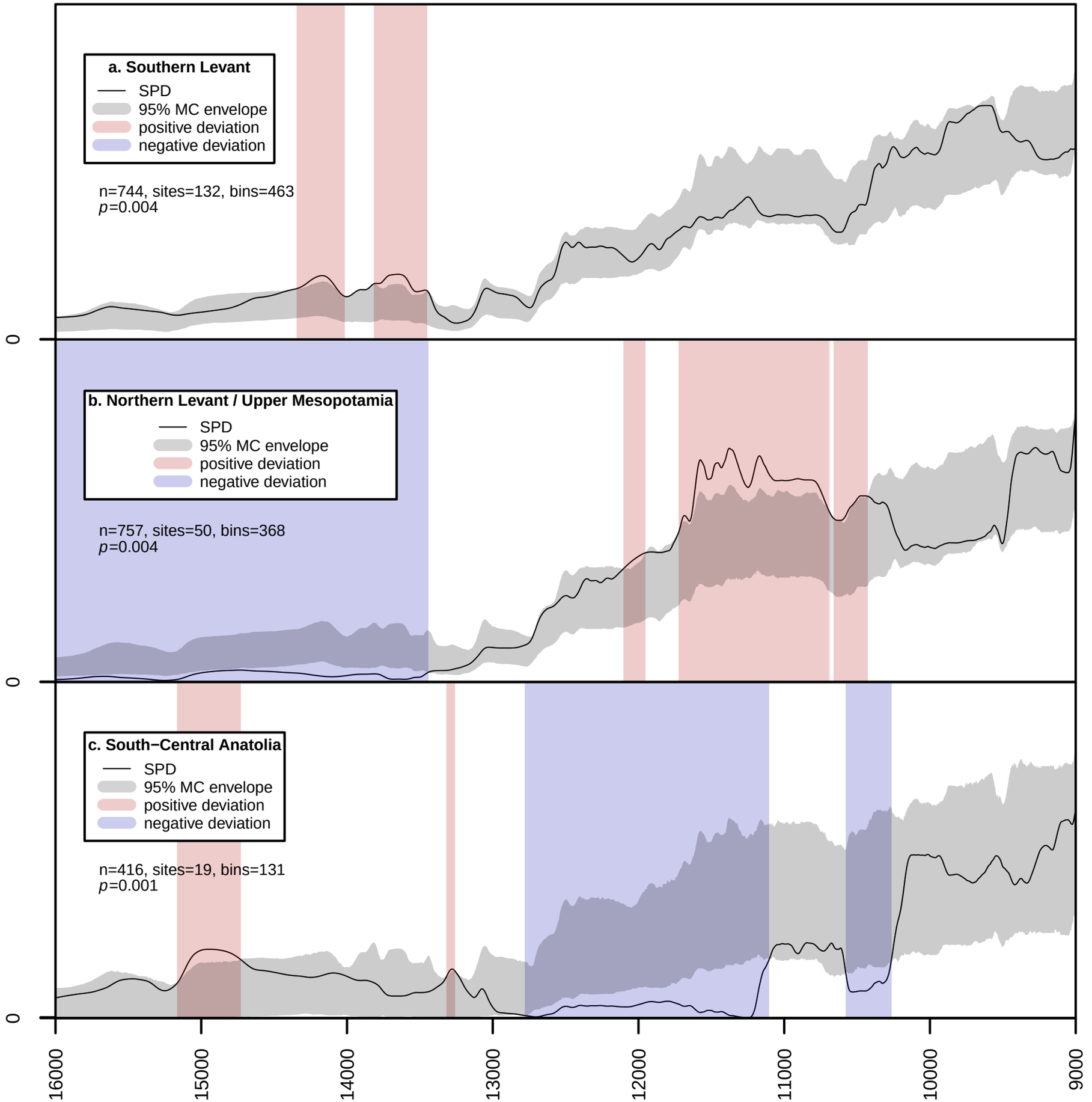
a. Southern Levant
SPD
95% MC envelope
positive deviation
negative deviation
n=744, sites=132, bins=463
p=0.004
b. Northern Levant / Upper Mesopotamia
SPD
95% MC envelope
positive deviation
negative deviation
n=757, sites=50, bins=368
p=0.004
c. South−Central Anatolia
SPD
95% MC envelope
positive deviation
negative deviation
n=416, sites=19, bins=131
p=0.001
0
0
0
16000
15000
14000
13000
12000
11000
10000
9000

Modelled climatic limits on cereal growth.
Areas with >= 20mm monthly precipitation and mean winter temperature >= -2ºC in yellow.

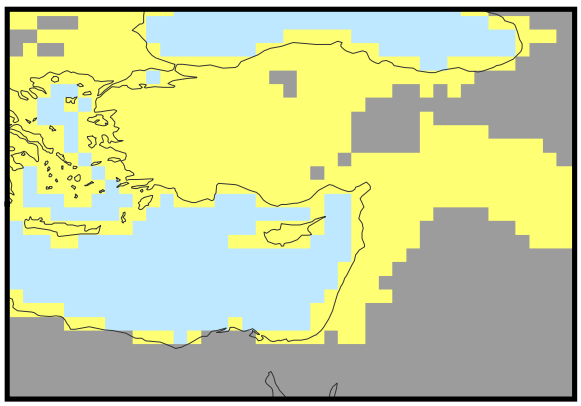

Holocene

Mean winter temperature: Modern (1901 - 1950)

Mean monthly precipitation 1901 - 1950

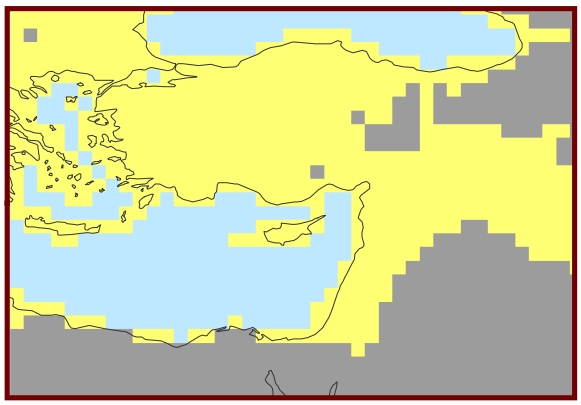

Early Holocene

Mean winter temperature: Modern +1ºC

Mean monthly precipitation: 130% modern

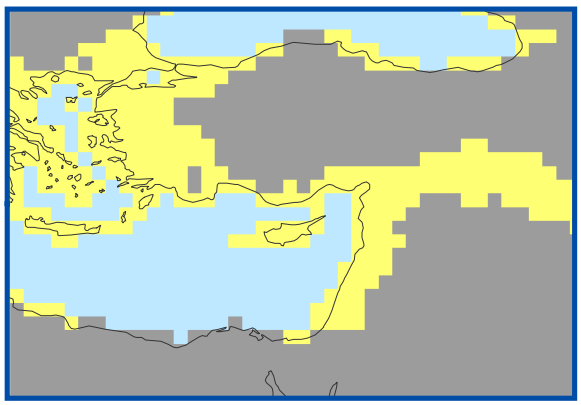

Younger Dryas stadial

Mean winter temperature: Modern -4ºC

Mean monthly precipitation: 75% modern

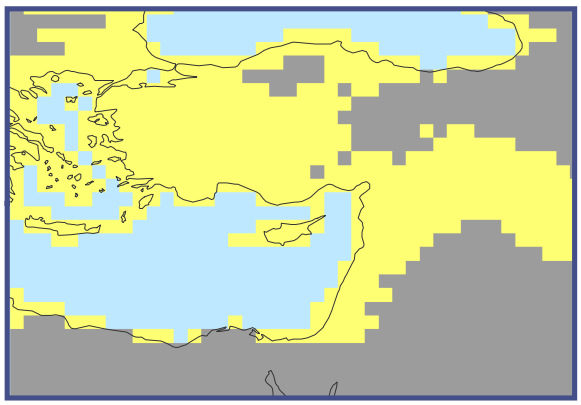

Late Glacial interstadial

Mean winter temperature: Modern -1ºC

Mean monthly precipitation: 120% modern

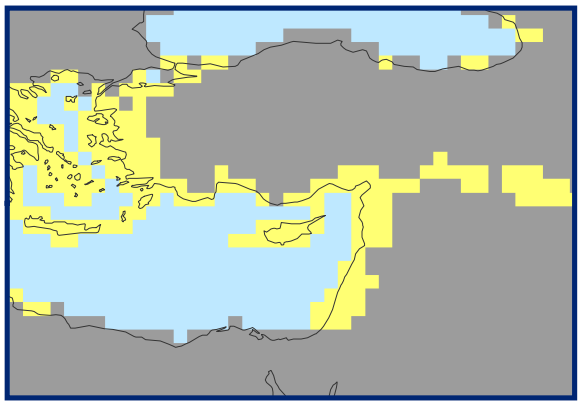

Glacial (H1)

Mean winter temperature: Modern -7ºC

Mean monthly precipitation: 60% modern

Modelled precipitation

Mean mm/month

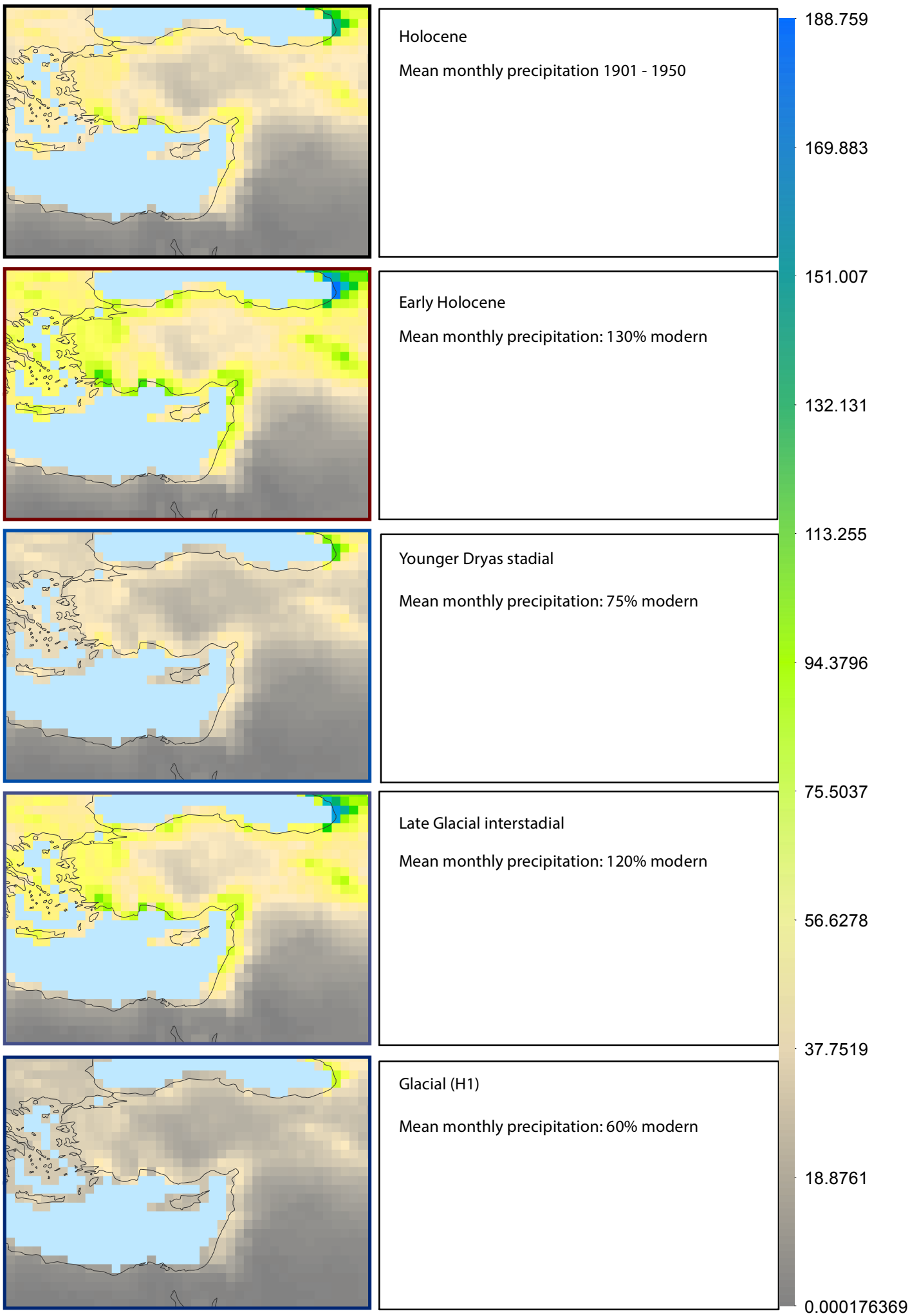

Mean monthly average temperature

Mean monthly average temperature (Dec - Feb)

Table S1: Stable isotope records used in this study

Site	**Type**	**References**
Zeribar, NW Iran	Lake	Stevens et al., 2001
Van, E Anatolia	Lake	Wick et al., 2003; Kwiecien et al., 2014
Eski Acıgöl, C Anatolia	Lake	Roberts et al., 2001
Akgöl, C Anatolia	Lake	Leng et al., 1999
Sofular, NW Anatolia	Cave	Göktürk et al., 2011
Soreq, Israel	Cave	Bar-Matthews et al., 1997 (and updates)
Jeita, Lebanon	Cave	Cheng et al., 2015
Dim, S Anatolia	Cave	Ünal-İmer et al., 2015
LC21, Aegean Sea	Marine	Grant et al., 2012
GISP2 (Greenland)	Ice core	Grootes and Stuiver, 1997

Table S2: Pollen records used in this study

Site	**References**
Zeribar, NW Iran	van Zeist and Bottema, 1991
Urmia, NW Iran	Bottema 1986
Van, E Anatolia	Wick et al., 2003
Eski Acıgöl, C Anatolia	Roberts et al., 2001; Woldring and Bottema, 2003
Akgöl, C Anatolia	Bottema and Woldring 1984
Ghab, NW Syria	Bottema and van Zeist 1981
Hula, Israel	Baruch and Bottema, 1991, 1999, chronology based on Meadows, 2005
Aammiq, Lebanon	Hajar et al., 2008; Cheddadi and Khater, 2016
Chamsine, Lebanon	Hajar et al., 2010; Cheddadi and Khater, 2016
Al Jourd, Lebanon	Cheddadi and Khater, 2016

Table S3: Changing proportions of woody plants by site and time period from archaeological charcoals

	Nahal Neqarot[1]	WF16[2]	Ma'aleh Ramon[1]	Abu Salem[1]	Saflulim[1]	Ramat Harif[1]	el-Hemmeh (PPNA)[7]	Dhra'[3]	Tell Qarassa N[4]	Tell es-Sultan[5]	'Ain Ghazal[6]	Basta[6]	el-Hemmeh (LPPNB)[7]
Juniperus	82.72	57.58	40.0									66	
Pistacia		3.16	58.0	99.95	61.59	99.62	70.71	X	59.48		<3	73	6.30
Quercus deciduous										?	>43		
Quercus evergreen		2.17					2.99	X	+	?	<3	4	0.65
Amygdalus/Prunus			0.20	0.02			2.84		37.25	X		11	1.94
Maloideae							0.16			X	X		0.48
Salicaceae		15.51					7.56	X	0.65	X	X	X	20.52
Tamarix	0.26	7.14					0.63	X		X	X	X	14.70
Fraxinus							1.57	X		X	X	X	34.73
Chenopodiaceae	0.79	3.99	0.40				7.24	X		X			6.30
Total ID charcoal	**382**	**2534**	**500**	**6620**	**138**	**6766**	**635**	**?26**	**153**	**~160**	**~1300**	**~1535**	**619**
Archaeological period	**Pre-Natufian**	**PPNA**	**Natuf**	**Harifian**	**Late Natufian**	**Harif**	**PPNA**	**PPNA**	**EPPNB**	**PPN**	**PPNB**	**Late PPNB**	**LPPNB**
Climate phase	**H1 (+ LGM)**	**E Hol 1 + YD**	**Younger Dryas**	**YD**	**Younger Dryas**	**YD**	**E Hol 1**	**E Hol 1**	**E Hol 1**	**E Hol 1/2**	**E Hol 2**	**E Hol 2**	**E Hol 2**
Age ka BP	**15.6-18.0 (+ 21-22)**	**10.3-12.5**	**11.7-12.5**	**11.6-12.5**	**12.8-13.0**	**11.7-12.5**	**10.5-11.1**	**10.5-11.0**	**10.0-10.6**		**8.5-9.9 (-10.4)**	**8.7-9.5**	**~9.0**
Location	**Negev highlands**	**S Jordan**	**Negev highlands**	**Negev**	**Negev**	**Negev**	**SE Jordan rift**	**SE Jordan rift**	**S Syria**	**Jordan rift**	**Trans-Jordan hills**	**S Jordan**	**S Jordan rift**

Table S3a: Key woodland taxa representation in published anthracological assemblages from late Pleistocene and early Holocene sites in the southern Levant – Taxa frequencies are expressed as % fragment counts (decimal numbers), or ubiquity scores (% presence, expressed as integer numbers). X denotes presence in charcoal assemblages with uncertainty regarding the precise quantitative value of the taxa reported in the published data. Total ID charcoal values represent identified charcoal fragment counts (integer numbers) or numbers of samples examined

(N=number of samples) and are reported only when included in published anthracological datasets. Dominant taxa are highlighted in grey. Data sources: [1]Baruch and Goring-Morris, 1997; [2]Austin, 2007; [3]Asouti, previously unpublished charcoal identifications produced for ^{14}C dating of handpicked specimens; [4]Arranz 2011 & personal communication 2014; [5](=Jericho) Western, 1971, 1983 hand-picked charcoals; [6]Neef 2004a-b; [7]Asouti et al. 2015 (‘Ain Ghazal: ubiquity scores were calculated by combining hand-picked and flotation samples; Western (1983) reported the presence of some oak charcoals from PPN deposits at Jericho, without specifying if they are evergreen or deciduous; Basta ubiquity scores were re-calculated from the published datasets on the basis of a sample population including only flotation samples that contained charcoal; other quantification methods employed by Neef in the analysis of the Basta charcoals such as % frequency measured by volume (ml) and % ubiquity calculated on the basis of all archaeobotanical samples including those that did not contain charcoal, were not taken into account) (modified after Asouti et al. 2015)

	Pınarbaşı Epipalaeolithic[1]	Pınarbaşı 9th-7th mill. cal BC[2]	Boncuklu[3]	Aşıklı höyük[4]	Can Hasan III[5]	Çatalhöyük East[6]
Quercus		0.36	5.06	X	+	40.13
Juniperus	30.32	0.04	0.36		++	21.58
Pistacia	3.72	15.57	2.66	X	++	1.48
Maloideae	11.17				+	0.91
Amygdalus/Prunus	50.53	79.83	14.61		+++	2.07
Celtis	1.06	1.17			++	3.86
Ulmus					+	2.41
Ulmaceae	0.53		1.56		++	9.72
Salicaceae	1.06		67.75	X	++	12.41
Fraxinus	1.60	0.27				2.78
Tamarix						0.16
Chenopodiaceae						0.43
Total charcoal ID	**188**	**4740**	**243**	**(N=16)**	**(N=97)**	**6312**
Archaeological period	**Epi-Pal**	**Aceramic Neolithic**	**Aceramic Neolithic**	**Aceramic Neolithic**	**Aceramic Neolithic**	**Ceramic Neolithic**
Climate phase	**B/A**	**E Hol 1 / 2**	**E Hol 1 / 2**		**E Hol 2**	**E Hol 2**
Age ka BP	**13-14.8 (+ 15.6)**	**9.6-11.0**	**9.7-10.2**		**8.6-9.6**	**8.2-9.3**
Location	**Konya**	**Konya**	**Konya**	**Cappad-ocia**	**Konya**	**Konya**

Table S3b: Key woodland taxa representation in published anthracological assemblages from late Pleistocene and early Holocene sites in central Anatolia – for an explanation of the reporting format see Table 1a. Data sources: [1]Baird et al., 2013; [2]Asouti, 2003; Asouti and Kabukcu, 2014; [3]Asouti and Kabukcu, 2014 (unpublished Boncuklu charcoal identifications not included); [4]Woldring and Cappers, 2001; [5]Willcox, 1992; [6]Asouti and Kabukcu, 2014 (unpublished charcoal identifications from Çatalhöyük East and Çatalhöyük TP Area not included) (relative taxon scoring scale for the Can Hasan III data is reported as defined by Willcox, 1992: + = presence in 1-25% of samples; ++=25-50%; +++=50-75%, ++++=75-100%).

	Çayönü[1]	Cafer höyük[2]	Göbekli Tepe[3]	Körtik Tepe[4]	Hallan Çemi[5]	M'lefaat[6]	Qermez Dere[7]	Chogha Golan[8]	Ganj Dareh[9]	Tepe Abdul Hosein[10]
Quercus deciduous	++++	++	0.6	X	X	2.84				
Pistacia	+++	+	63.4	X	X	5.69	X	37.22	++	++++
Celtis/Pistacia									++++	
Amygdalus/Prunus	+++		36.0	X	X			3.31	++	+++
Maloideae				X				0.08		+
Celtis		+		X					+	
Salicaceae		+++		X	X	42.65		33.09	++++	++
Tamarix	+++			X		28.91	X	21.51		+
Fraxinus	+++	+		X	X	15.17				
Chenopodiaceae							X	1.65		+
Total ID charcoal	**(N=60)**	**(N=84)**	**164**	**1487**	**125**	**211**	**>15?**	**1209**	**(N=76)**	**(N=20)**
Archaeological period	**PPNA/B**	**PPNB**	**PPNA/B**	**PPNA**	**PPNA**	**E aceramic Neo**		**Aceramic Neo**		
Climate phase	**E Hol 1 / 2**	**E Hol 2**	**E Hol 1 / 2**	**YD E Hol 1**	**EH 1**	**EH 1 (+YD?)**		**E Hol 1 / 2**		
Age ka BP	**(8.9) 9.8-10.9 (12.7)**	**(8.8) 9.3-10.1**	**(8.4) 9.4-11.5**	**11.2-12.2**	**11.3-11.7**	**10.9-11.4 (12.8)**		**9.7-10.7**		
Location	**SE Anatolia**	**SE Anatolia**	**SE Anatolia**	**SE Anatolia**	**SE Anatolia**	**N Iraq**		**W Iran**		

Table S3c: Key woodland taxa representation in published anthracological assemblages from late Pleistocene and early Holocene sites in southeast Anatolia and the Zagros – for an explanation of the reporting format see Table 1a. Data sources: [1]van Zeist, 1972; van Zeist and de Roller 1991/2; [2]Willcox, 1991; [3]Neef, 2003; [4]Riehl et al. 2012; [5]Rosenberg et al., 1998; [6]Savard et al., 2003; [7]Watkins et al., 1989; Savard et al., 2003; [8]Riehl et al. 2015; [9]van Zeist et al., 1984 (including both hand collected and flotation samples; from the authors' discussion of the evidence it can be surmised that most of the fragments identified as *Celtis/Pistacia* are likely to represent *Pistacia* hence the highlighting of

Pistacia as a dominant taxon); [10]Willcox, 1990 (relative taxon scoring scale for the Can Hasan III, Ganj Dareh and Tepe Abdul Hosein data is reported as defined by Willcox, 1992: + = presence in 1-25% of samples; ++=25-50%; +++=50-75%, ++++=75-100%)

	Abu Hureyra 1[1]	Mureybet I-III[2]	Jerf el Ahmar[3]	Dja'de[3]	Tell Halula MPPNB[3]	Tell Halula LPPNB[3]
Quercus deciduous	X	X	X	X	X	X
Pistacia	X	X	X	X	X	X
Amygdalus/Prunus	X	X?	X	X	X	X
Maloideae					X	
Ulmaceae	X		X		X	X
Salicaceae	X	X	X	X	X	X
Tamarix	X	X	X	X	X	X
Fraxinus	X		X	X	X	X
Chenopodiaceae	X	X	X	X	X	X

Table S3d: Key woodland taxa representation in published anthracological assemblages from late Pleistocene and early Holocene sites in northern Syria – for an explanation of the reporting format see Table 1a. Data sources: [1]Roitel and Willcox, 2000; [2]Savard et al., 2003; Willcox, 2008; pers. comm.

Table S4: Charcoal data by time period and region used for figure 5

Climate phase	**H1**	**B/A**	**YD**	**E Hol 1**	**E Hol 2**
Mean age ka BP	16	13.7	12.4	11	9.6
S Levant					
Archaeological period	"Kebaran"	Early Natufian	Late Natuf/Harif	PPNA-EPPNB	M-LPPNB
Number of sites	1	0	5	3	3
Juniperus	16.0	13.7	12.4	11.0	9.6
Pistacia	1.0	0.0	5.0	3.0	3.0
Quercus deciduous	82.7	nd	19.5	19.2	22.0
Amygdalus/Prunus	0.0	nd	64.5	44.5	27.4
Riparian taxa	0.0	nd	0.0	0.0	14.3
Other	0.0	nd	0.0	13.4	4.3
N Levant/SE Anatolia					
Archaeological period	Epi-Pal	Epi-Pal	Epi-Pal	E aceramic Neo	Aceramic Neo
Number of sites	0	0	0	4	4
Juniperus	nd	nd	nd	0.0	0.0
Pistacia	nd	nd	nd	30.3	30.2
Quercus deciduous	nd	nd	nd	8.4	13.9
Amygdalus/Prunus	nd	nd	nd	13.6	13.6
Riparian taxa	nd	nd	nd	42.8	34.9
S C Anatolia					
Archaeological period	Epi-Pal	Epi-Pal	Epi-Pal	L Epi-Pal / E aceramic Neo	Aceramic Neo
Number of sites	0	1	0	2	4
Juniperus	nd	30.3	nd	0.2	3.4
Pistacia	nd	3.7	nd	9.1	8.1
Quercus deciduous	nd	0.0	nd	2.7	12.1
Amygdalus/Prunus	nd	50.5	nd	47.2	30.1
Riparian taxa	nd	3.2	nd	34.8	34.9
Other	nd	12.2	nd	6.0	11.4

Table S5: Palaeo-temperature and palaeo-precipitation estimates used for climate scenario modelling

Time interval	Age ka BP	Sea-surface temperatures (°C difference)				Mean annual precipitation (difference)		
		Ionian sea Emeis et al 2000	E Med Essallami 2007	Used here		Soreq	Eski Acıgöl	Used here
Early Holocene	11.0±0.5	-4	1	1		53%*	22%	30%
Late Glacial stade	12.5±0.5	-8	-2	-4		-6%	-25%	-25%
Late Glacial interstade	14.5±1.0	-1	0	-1		31%	41%	20%
Heinrich 1	16.0±1.0	nd	-6	-7		nd	-38%	-40%

*7.5 ka BP